(NASA-CR-182959) APPLICATION OF THE MODAL ANALYSIS APPROACH TO TRANSIENT THERMAL PROBLEMS (Swales and Associates) 65 p

N90-70420

Unclas

00/64 0234047

LIBRARY COPY

AUG 1 19

LANGLEY RESEARCH CENTER
LIBRARY NASA
HAMPTON, VIRGINIA

SWALES & ASSOCIATES, INC.

#234047

APPLICATION OF THE MODAL ANALYSIS APPROACH TO TRANSIENT THERMAL PROBLEMS

October 1981

AUG 1 1982

LANGLEY RESEARCH CENTER
LIBRARY NASA
HAMPTON, VIRGINIA

Prepared by

J. Anderes
Swales and Associates, Inc.

Under Subcontract SSD-81-100

to

COMPUTER SCIENCES CORPORATION

for

Contract NAS 5-26299

to the

NATIONAL AERONAUTICS AND SPACE ADMINISTRATION

GODDARD SPACE FLIGHT CENTER

TABLE OF CONTENTS

Section 1 - Introduction. 1-1

Section 2 - Modal Formulation of the Transient Thermal Problem 2-1

2.1 CAVE. 2-2
2.2 Structural Analogy. 2-5

Section 3 - Implementation of a General Modal Formulation of the Transient Thermal Problem . . . 3-1

Section 4 - Transient Thermal Analysis Examples. . . . 4-1

4.1 One-Dimensional Conduction Problem. 4-1
4.2 JPL Antenna Problem 4-19

Section 5 - Conclusion. 5-1

Appendix A - JPL Antenna Thermal NASTRAN Data Deck. . . A-1

References. R-1

LIST OF ILLUSTRATIONS

Figure

1 One-Dimensional Conduction Problem 4-2
2 One-Dimensional Conduction Problem Thermal Equation 4-3
3 One-Dimensional Conduction Problem--First Mode Shape. 4-4
4 One-Dimensional Conduction Problem--Response to First Mode Temperature Distribution. 4-6
5 Nodal Temperature Responses, 10 Mode Solution. . . . 4-7
6 Nodal Temperature Responses, 6 Mode Solution 4-8
7 Structural Analogy to One-Dimensional Conduction Problem. 4-14
8 First 3 Modes--Conduction Slab Only. 4-15
9 Nodal Temperature Responses--Modes Deleted After 3 Time Constants 4-16
10 Nodal Temperature Responses--Modes Deleted After 5 Time Constants 4-17
11 Slab Nodal Temperature Responses--Integration Time Step 10 Times Larger Than Nominal. 4-18
12 JPL Antenna Thermal Model. 4-20
13 Interior Dish Nodal Temperature Responses. 4-21
14 Feeder Nodal Temperature Responses 4-22
15 Pedestal Nodal Temperature Responses 4-23
16 Color Graphics Display of First JPL Antenna Thermal Mode 4-25
17 Pedestal Nodal Temperature Responses--36 Mode Solution 4-27
18 JPL Antenna Model Run Times. 4-29

LIST OF TABLES

Table

1 Eigenvalues and Time Constants for the One-Dimensional Conduction Problem 4-5
2 Modal Contributions to Slab Final Temperatures . . . 4-11
3 Slab Only Time Constants. 4-13
4 JPL Antenna Time Constants. 4-24
5 JPL Mode Classification 4-28

SECTION 1 - INTRODUCTION

Conventional techniques available for structural, thermal and control system analysis may well be inadequate for the analysis of the large space structures now being envisioned for future space applications. This report presents the results of studying one aspect of this problem.

A number of recent papers have been published which present a modal solution approach to the transient thermal analysis problem. Two in particular are considered in this report. In the first [1], a generalized approach for the solution of thermally induced instabilities is formulated in order to perform the analysis of coupled structural and thermal systems. The second paper [2] addresses the application of two-dimensional transient heating of hypersonic vehicles, specifically establishing a code to improve run time efficiency.

The purpose of this report is to present an evaluation of the modal formultions of the thermal transient analysis problem. A computational technique is then presented for solving such problems. The results of testing this technique on representative problems to ascertain potential benefits and disadvantages is then given, along with conclusions and recommendations for pertinent follow-on activities.

SECTION 2 - MODAL FORMULATIONS OF THE TRANSIENT THERMAL PROBLEM

This section contains the evaluation of two specific modal formulation approaches. Special attention is given to mathematical derivation and generality.

In order to have a common base of notation, the general thermal transient equation is, for the purposes of this report

$$B\dot{T} + KT + R(T + T_a)^4 = P + N \tag{1}$$

where T = vector of nodal temperatures

B = diagonal (lumped) matrix of system heat capacitance coefficients

K = symmetric matrix of system heat conduction coefficients

R = matrix relating radiative heat flows to nodal temperatures

T_a = converts T to an absolute temperature scale

P = time dependent applied heat flows

N = nonlinear heat flows that depend on temperature

Note that this notation is not the standard formulation used by thermal analysts who nominally write thermal balance difference equations at each node. It is, in fact, nearly equivalent to the general equation found in NASTRAN [3] in its heat transfer analysis rigid formats. It was chosen as a basis in order to point out thermal and structural analogies.

The NASTRAN Thermal Analyzer (NTA) is a finite element analysis method in which the unknowns are temperatures at discrete points. The heat conduction matrix, K, and the heat capacity matrix, B, are formed from element properties. The

K matrix may also include surface heat convection or linearized radiation. The applied heat flow vector, P, is associated with either surface heat transfer or heat generated inside the volume heat conduction elements. Radiation from a distant source is treated as a prescribed heat flux. Radiation exchange between surfaces is contained in the $R(T + T_a)^4$ nonlinear term. N contains nonlinear heat flows due to temperature dependent surface convection and heat conductivity. An excellent report fully detailing the theory and practical aspects of using NTA is given in Reference 4.

2.1 CAVE

CAVE (Conduction Analysis Via Eigenvalues) is a standalone computer code generated to make the prediction of temperatures within the thermal protection systems of hypersonic vehicles more convenient and efficient. In the CAVE approach, a transient thermal event or trajectory is divided into intervals of time over which the heat capacitance, conductance, and thermal load matrices are constant. Linearized radiation heat transfer at the surface can be included by modifying the convection coupling terms. Therefore, the equation to be solved is, within a specified time interval,

$$B\dot{T} + KT = P \tag{2}$$

where the B, K, and P matrices are all constant with respect to temperature and time. There thus exists a closed form solution to this problem, the derivation of which is shown in Appendix F of the CAVE report. A brief reformulation of the derivation is shown in the following steps.

1. Perform coordinate transformation $T = B^{-1/2}x$

$$B^{1/2}\dot{x} + KB^{-1/2}x = P \tag{3}$$

2. Multiply equation (3) by $B^{-1/2}$

$$\dot{x} + B^{-1/2}KB^{-1/2}x = B^{-1/2}P$$

or

$$\dot{x} + Ax = B^{-1/2}P \tag{4}$$

3. Perform second coordinate transformation $x = B^{1/2}y$

$$B^{1/2}\dot{y} + AB^{1/2}y = B^{-1/2}P \tag{5}$$

4. Multiply equation (5) by $B^{-1/2}$

$$\dot{y} + B^{-1/2}AB^{1/2}y = B^{-1}P$$

or

$$\dot{T} + NT = B^{-1}P \tag{6}$$

since

$$T = B^{-1/2}x = B^{-1/2}B^{1/2}y = y$$

5. The homogeneous solution to equation (6) is an exponential function

$$T_h = ce^{Nt} \tag{7}$$

6. The nonhomogeneous solution to equation (6) is a constant

$$T_\infty = N^{-1}B^{-1}P \tag{8}$$

7. Total solution to equation (6) is

$$T = ce^{Nt} + T_\infty \tag{9}$$

At $t = 0$, $T = T_0$

Therefore

$$c = T_0 - T_\infty$$

Thus

$$T(t) = (T_0 - T_\infty)e^{Nt} + T_\infty \tag{9}$$

The rest of the derivation in the CAVE report is spent in evaluating the term e^{Nt} via algebraic manipulations. It is shown through a number of steps, which need not be repeated here, that

$$\begin{aligned} e^{Nt} &= e^{B^{-1/2}AB^{1/2}t} \\ &= B^{-1/2}\phi e^{\Lambda t}\phi^T B^{1/2} \end{aligned} \tag{10}$$

where Λ = diagonal matrix containing the eigenvalues λ_j of matrix A

ϕ = eigenvectors of matrix A where $\phi^T A\phi = \Lambda$, $\phi^T\phi = I$

Thus, the final modal formulated solution becomes

$$T(t) = B^{-1/2}\phi e^{\Lambda t}\phi^T B^{1/2}(T_0 - T_\infty) + T_\infty \tag{11}$$

Another way to express equation (11) for node i is

$$T_i(t) = T_{\infty_i} + \sum_j^n c_{ij}e^{\Lambda_j t} \tag{12}$$

where n is the number of dominant terms. It is noted that, for a given number of terms, there is a minimum time period required to achieve a certain accuracy. This aspect of the problem will be discussed in more detail in Section 4.

Clearly, the CAVE program solves a somewhat restricted problem in an efficient manner. It is also clear that a very informed user is required to choose optimal values for the trajectory time intervals and the correct number of dominant modes in order to achieve a specified accuracy level.

2.2 STRUCTURAL ANALOGY

The impetus for this report was generated by the H. P. Frisch paper "Thermally Induced Response of Flexible Structures: A Method for Analysis" [2]. It presents an analysis procedure for coupling thermal and structural modes in a very general and straight forward manner.

The general matrix equation which Frisch derives from the thermal balance equation at each node, is

$$B\dot{T} + K'u = P$$

This equation is essentially identical to the NTA linear formulation in which the K' matrix contains, in additio

heat conductances, linearized radiation terms developed as follows

$$
\begin{aligned}
RT^4 &= R\left[T_E + \Delta T\right]^4 \\
&= R\left[T_E^4 + 4T_E^3\Delta T + 2T_E^2\Delta T^2 + \ldots\right] \qquad (14) \\
&= R\left[T_E^4 + 4T_E^3\Delta T\right]
\end{aligned}
$$

Here, the terms are linearized about the average mean temperatures at each node T_E. The right hand side vector, P, contains the constant RT_E^4 and KT_E terms as well as applied time dependent heat fluxes.

The modal solution to the homogeneous form of equation (13) is developed by considering a solution of the form

$$T = \phi e^{-\lambda t} \qquad (15)$$

Therefore, the eigenvalue problem becomes

$$(\lambda B - K)\phi = 0 \qquad (16)$$

The solution to this eigen-analysis problem may be formulated as a coordinate transformation

$$T = \phi Q$$

where $\phi^T B \phi = I$ (identity matrix)

$\phi^T K \phi = \Lambda$ (diagonal matrix of eigenvalues λ)

Therefore, the uncoupled system equations become

$$\dot{Q} + \Lambda Q = \phi^T P \qquad (17)$$

or for the ith equation

$$\dot{q}_i + \lambda_i q_i = \sum_j \phi_{ji} P_j$$

The solution Q(t) of these equations via integration may then be back transformed to temperature via

$$T(t) = \phi Q(t) \tag{18}$$

Potential CPU savings over normally fully coupled integration may result due to both diagonal matrix integration (no forward-backward substitution) and modal truncation. This was not, however, the purpose of the Frisch paper which instead went on with a presentation of the coupling of structural and thermal modes in order to simulate thermally driven structures. The final sections of this report detail the investigation into the potentials of modal thermal solutions which the Frisch paper did not address.

SECTION 3 - IMPLEMENTATION OF A GENERAL MODAL FORMULATION OF THE TRANSIENT THERMAL PROBLEM

A third and more general approach to solving transient thermal analysis problems in the modal domain begins with the NTA equivalent of equation (1)

$$B\dot{T} + K'T = P + N \tag{19}$$

where

$$N = R\left(4(T_E + T_a)^3 T - (T + T_a)^4\right)$$

$$K' = K + R\left(4(T_E + T_a)^3\right)$$

As in the Frisch paper, the radiation terms are linearized about a user estimated final steady state temperature, T_F. However, the linearized terms are included on both sides of the equation and thus equation (19) is an exact representation of equation (1). The full nonlinear term is now incorporated on the right hand side in a forcing function role. It could easily include temperature-dependent terms as NTA does, but this was not incorporated at this time.

The modal solution to equation (19) is much the same as in the Frisch paper. The following steps depict the implementation process.

1. Perform coordinate transformation $x = T - T_0$ where T_0 is the initial vector of nodal temperatures

$$B\dot{x} + K'x = P + N - K'T_0 \tag{20}$$

2. Perform modal coordinate transformation $x = \phi Q$ where

$$\phi^T B \phi = I$$

$$\phi^T K' \phi = \Lambda$$

$$\dot{Q} + \Lambda Q = \phi^T P + \phi^T N - \phi^T K' T_0 \tag{21}$$

3. Integrate the uncoupled "dominant" equations (21). The integration package chosen is the same as that used in the Nastran coupled matrix transient thermal analyzer. It is related to the second-order Newmark-beta approach used in structural analysis, being both stable and efficient. The algorithm for equation (21) is

$$\left[\frac{I}{\Delta t} + \beta\Lambda\right] Q_{n+1} = \left[\frac{I}{\Delta t} - (1 - \beta)\Lambda\right] Q_n + \beta P_{n+1} + (1 - \beta) P_n + (1 + \beta) N_n - \beta N_{n-1} \tag{22}$$

Note that the matrices in brackets are diagonal, yielding a very efficient algorithm for this set of equations. The algorithm is started by setting

$$P_0 = K' T_0 - N_0$$

$$N_{-1} = N_0$$

4. Back transform from modal results to obtain physical temperatures

$$T(t) = \phi Q(t) + T_0 \tag{23}$$

This procedure was implemented in both the fully coupled and modal formulations in the FLAME program [5]. For simple problems such as the one-dimensional conduction problem in the next section, the entire problem can be formulated using FLAME commands. For more complex problems such as the JPL antenna model of the next section, a NTA run to create and output the B, K, R, and P matrices is made. DMAP instructions were also added to solve the associated eigenvalue problem and output the eigenvalues and mode shapes.

SECTION 4 - TRANSIENT THERMAL ANALYSIS EXAMPLES

In this section, two thermal transient problems are analyzed using the procedure presented in Section 3. Accuracy, efficiency and practicality are stressed. An assessment of physical interpretation of thermal eigenvalues and mode shapes for these problems is also included.

4.1 ONE-DIMENSIONAL CONDUCTION PROBLEM

The problem considered here is taken from Appendix A of the CAVE report. It is a 10-node network representing a uniform slab heated by convection on one face and perfectly insulated on the other. Figure 1 displayes the network, the system properties, dimensions and temperatures. Figure 2 gives the associated system matrices used in solving this problem. Note that the fluid connective coupling is included in the problem by means of a linear spring constant. Note also that for the uniform slab properties as given, this problem could be represented by only two nodes.

The modal formulation of this problem yields 10 eigenvalues and thermal mode shapes. These eigenvalues and mode shapes may be physically interpreted by considering a structural analogy. If an undamped structure is physically configured into one of its mode shapes and then released, it will vibrate indefinitely with that mode shape at the frequency of that mode. Likewise, if a structure is given an initial thermal distribution associated with one of its thermal mode shapes referenced to some mean temperature, the nodal temperatures will approach the mean temperature exponentially with a time constant equal to the reciprocal of the eigenvalue for that mode shape.

To show this, consider the slab model. Its eigenvalues and associated time constants are shown in Table 1. A plot of the first mode is shown in Figure 3 (maximum normalized to

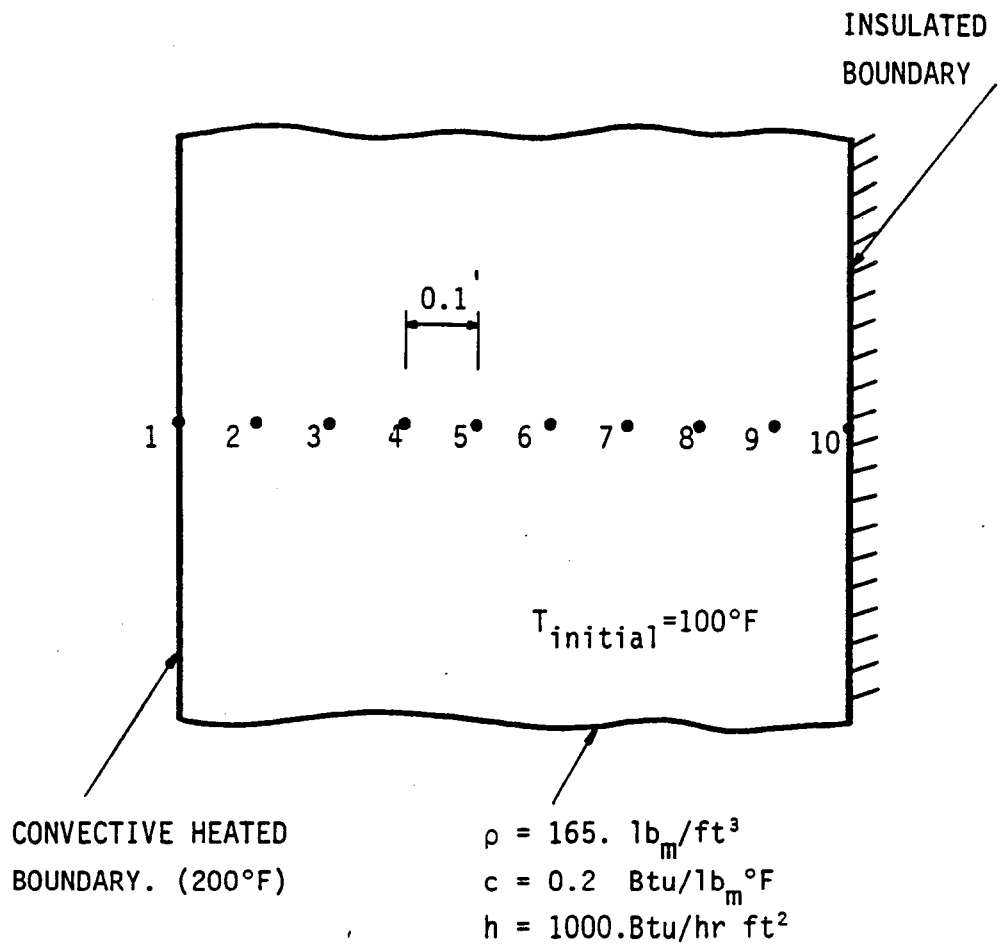

Figure 1. One-dimensional Conduction Problem

THERMAL EQUATION:

$$B\dot{T} + KT = P$$

where

$$B = \mathrm{diag}\ (1.65,\ 8*3.3,\ 1.65) \quad \mathrm{BTU/^{o}F}$$

$$K = \begin{bmatrix} 2000. & -1000. & 0. & & & \\ -1000. & 2000. & -1000. & & 0. & \\ 0. & -1000. & 2000. & & & \\ & & & \ddots & & \\ & & & & -1000. & \\ & 0. & & & 2000. & -1000. \\ & & & & -1000. & 1000. \end{bmatrix}$$

$$P = (200000.,\ 9*0.)^{T} \quad \mathrm{BTU/hr.}$$

Figure 2. One-Dimensional Conduction Problem Thermal Equation

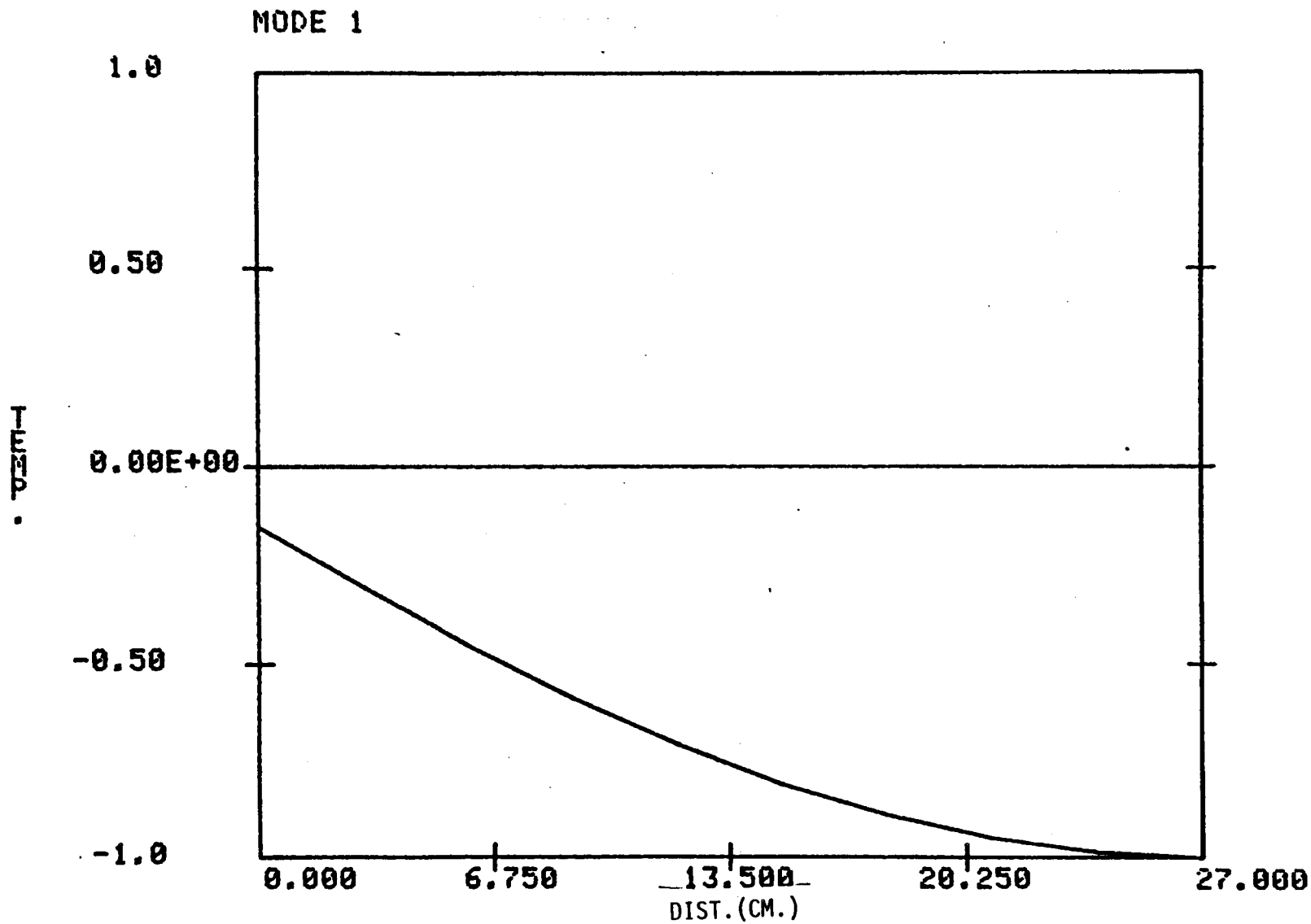

Figure 3. ONE-DIMENSIONAL CONDUCTION PROBLEM -- FIRST MODE SHAPE

±1°F). If the system is given an initial temperature distribution of that mode shape and then released with 0°F boundary conditions, Figure 4 displays how the temperatures at nodes 1, 5, and 10 behave. Note that they all approach 0°F at an exponential rate associated with the time constant of the first mode, 0.134 hour. Each modal temperature decays to 37% of its original temperature in one time constant, and to 5% of its original temperature in three time constants.

Table 1. Eigenvalues and Time Constants for the One-Dimensional Conduction Problem

Mode Number	Eigenvalue (hr^{-1})	Time Constant (hr)
1	7.47	.13385
2	67.26	.01487
3	185.1	.005404
4	352.5	.002837
5	552.7	.001809
6	763.2	.001310
7	958.2	.001044
8	1112.0	.000899
9	1119.0	.000834
10	1461.0	.000684

A plot of the response of nodes 1, 5, and 10 to the problem as formulated is shown in Figure 5. This plot was obtained using all ten modes. It agrees exactly with the full coupled solution approach and with the results as presented in the CAVE manual. A number of runs were made with less than ten modes with results shown in Figure 6 for six modes. It became apparent quickly that for this problem as formulated, all modes are required to give accurate representation of the final slab temperatures. This was not

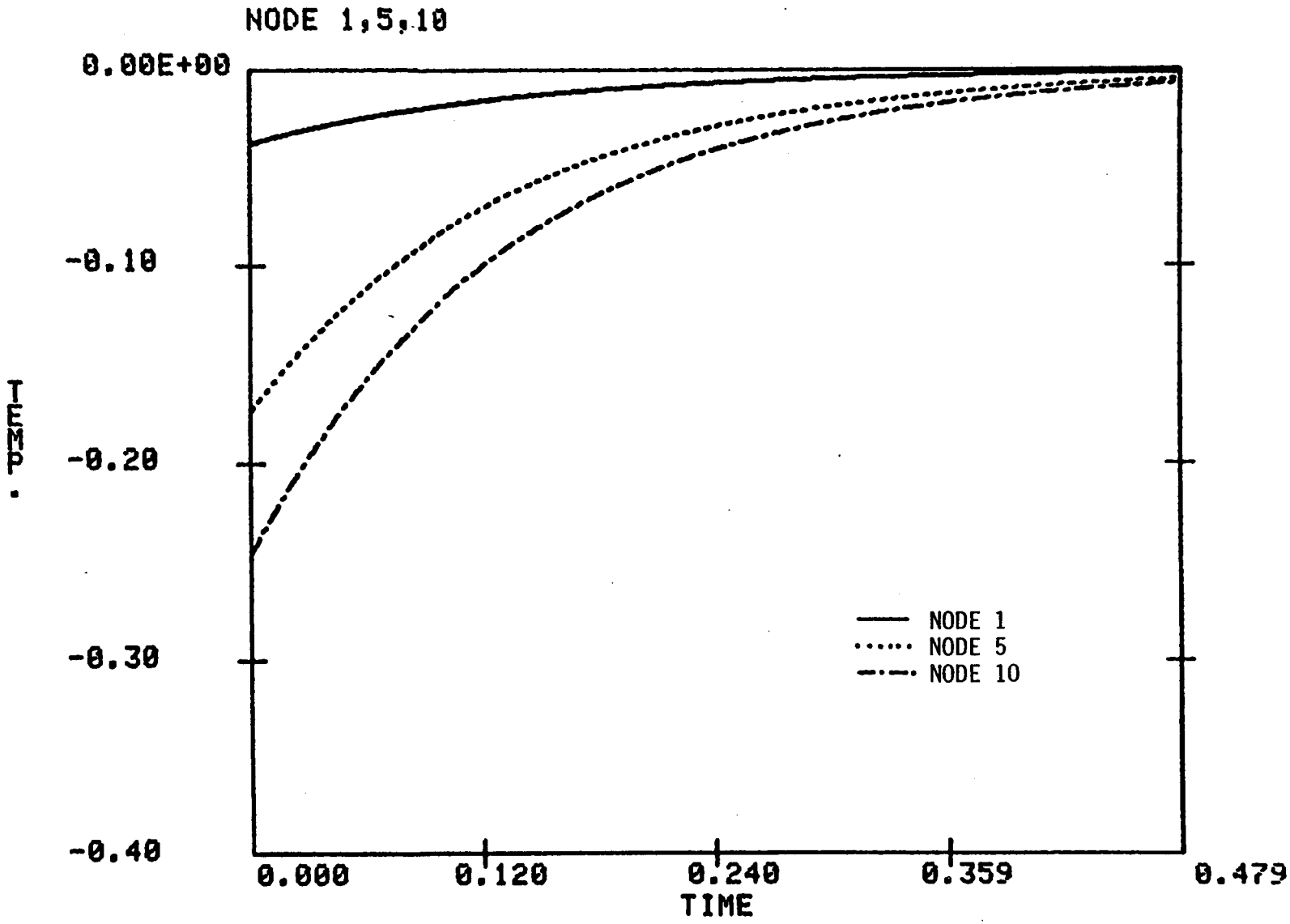

Figure 4. ONE-DIMENSIONAL CONDUCTION PROBLEM --- RESPONSE TO FIRST MODE TEMPERATURE DISTRIBUTION

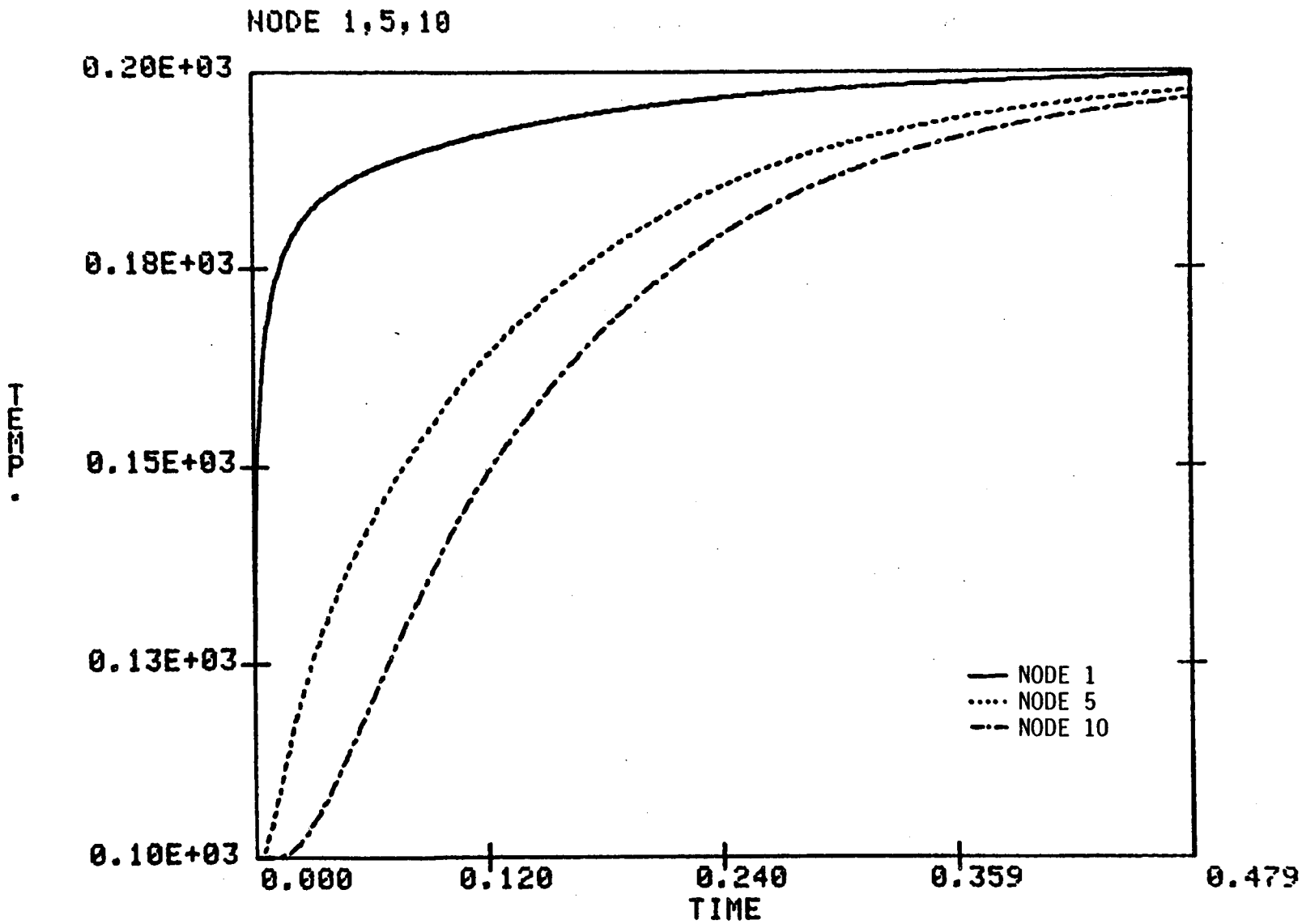

Figure 5. NODAL TEMPERATURE RESPONSES, 10 MODE SOLUTION

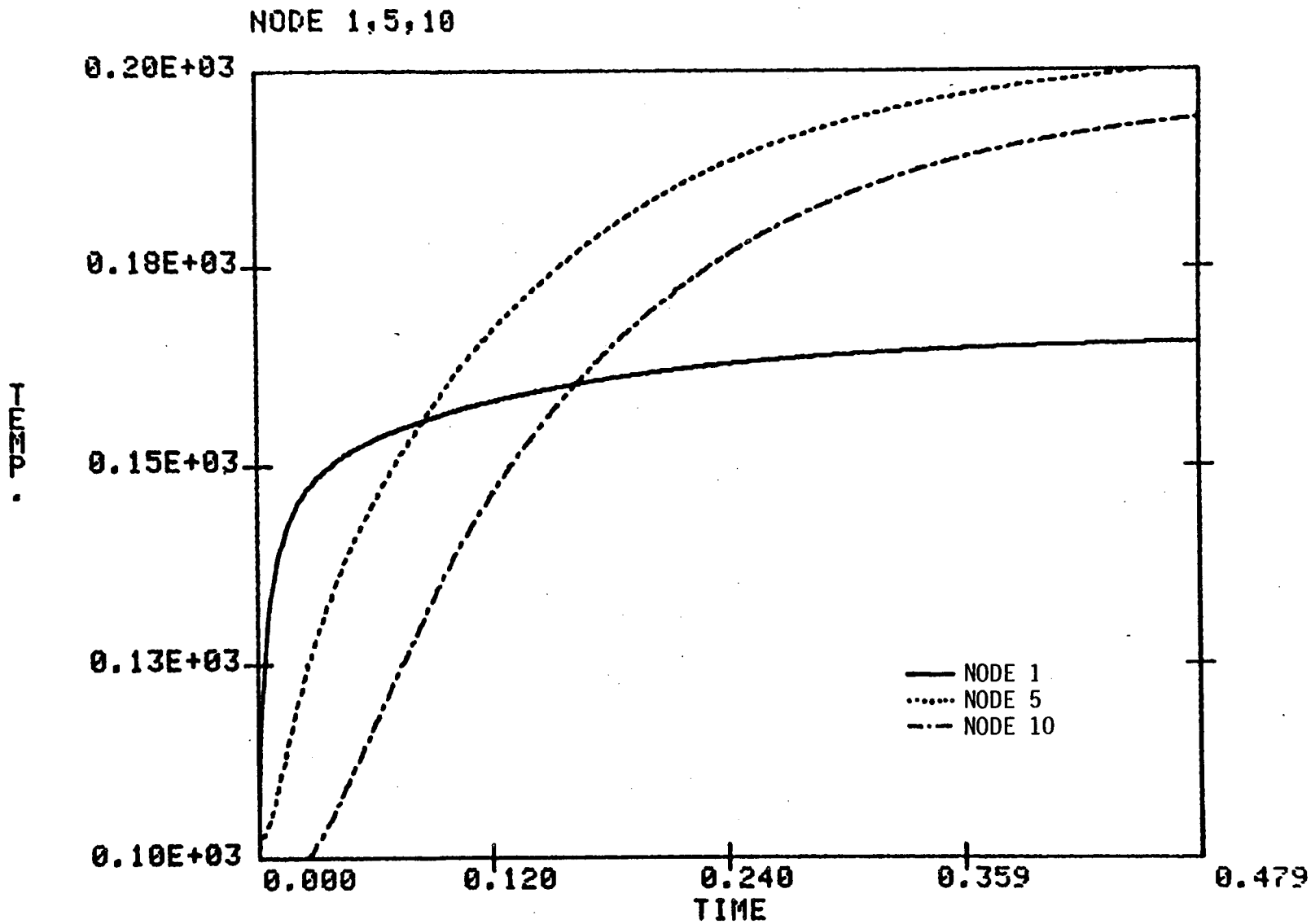

Figure 6. NODAL TEMPERATURE RESPONSES, 6 MODE SOLUTION

expected, especially since the CAVE documentation showed that only one mode gave the correct temperature response after approximately 0.08 hour. It must be recognized however that the CAVE formulation solves a very specific linearized problem with constant thermal loading, thus allowing a very specific exact solution representation.

In order to evaluate the "surprizing" results when modal truncation is used for this problem, consider the following solution steps:

1. Problem Formulation:

$$\dot{B}u + Ku = P$$

$$\dot{u}(0) = 0$$

$$u(0) = 0^{o}F \text{ (for clarity)}$$

$$P = [p, 0., 0., 0., 0., 0., 0., 0., 0., 0.]^T$$

2. Modal Formulation:

$$u = \phi q$$

$$\phi^T B \phi = I$$

$$\phi^T K \phi \doteq \text{diag } (\lambda_1, \ldots, \lambda_9, \lambda_{10})$$

$$\dot{Q} + \Lambda Q = Q^T P$$

3. ith modal equation:

$$\dot{q}_i + \lambda_i q_i = \sum_j \phi_{ji} P_j \qquad P_j = 0 \quad j \neq 1$$

$$P_j = p \quad j = 1$$

$$\dot{q}_i + \lambda_i q_i = \phi_{1i} p$$

4. Laplace Solution (step input):

$$q_i(t) = \frac{\phi_{1i}p}{\lambda_i}\left(1. - e^{-\lambda_i t}\right)$$

5. Back Transform to Temperature at ith node:

$$u_i(t) = \sum_j \frac{\phi_{ij}\phi_{1j}p}{\lambda_j}\left(1. - e^{-\lambda_j t}\right)$$

6. Final Steady State Temperature ($t \to \infty$):

$$u_i = \sum_j \frac{\phi_{ij}\phi_{1j}p}{\lambda_j}$$

Thus, the final steady state temperature at, for example node 1, becomes

$$u_1 = \left(\frac{\phi_{11}^2}{\lambda_1} + \frac{\phi_{12}^2}{\lambda_2} + \ldots + \frac{\phi_{1,10}^2}{\lambda_{10}}\right)p$$

The terms ϕ_{1j}^2/λ_j are the effective modal participation of each mode to the final steady state temperature at node 1. The modal participation of the jth mode at node i is a function of the product of the jth mode shape with the mode shape at the first node (where the load is applied) divided by the jth mode eigenvalue. Table 2 gives the corresponding contributions to the final temperatures (at 0.48 hour) at nodes 1, 5, and 10. The numbers for node 1 are especially revealing, for while λ_{10} is nearly 200 times greater than λ_1, $\phi_{1,10}^2$ is nearly 300 times

Table 2. Modal Contributions to Slab Final Temperatures

	Temperature At .48 Hour		
Mode	Node 1	Node 5	Node 10
1	37.0	170.0	240.0
2	32.0	56.0	-77.0
3	24.0	-26.0	40.0
4	17.0	-21.0	-24.0
5	13.0	9.0	15.0
6	9.0	13.0	-12.0
7	6.0	0.0	8.0
8	2.0	-6.0	-6.0
9	1.0	-1.0	2.0
10	59.0	2.0	0.0
	200.0	196.0	186.0

greater than ϕ_{11}^2 and thus the contribution of mode 10 at node 1 is about 1.5 times greater than that of mode 1.

The problem of modal truncation in this example is really a function of the way the convective boundary coupling is included in the model. The structural equivalent of this problem is shown in Figure 7. The structural dynamicist might well analyze this problem by considering not the modes of the beams plus the spring, but those of the free-free beam alone and then recoupling the system equations using the ΔK [6] solution approach. This should lead to greater flexibility in modal truncation. For example, the eigenvalues and time constants for the conducting slab alone are given in Table 3. The mode shapes all have the same maximum value, some of which are shown in Figure 8. It is likely, because of the extremely high value for the first mode time constant, that it will easily dominate the system solution.

Other analysis techniques for this problem are also possible. For example, modal equations can be deleted during integration after a specified number of time constants have passed in order to lower CPU run time. Figure 9 shows the results for deleting equations after 3 time constants. Five time constants seems to be the appropriate number for accurate results, as Figure 10 clearly shows.

Yet another parameter which can be changed is the integration step size. The method incorporated is stable for large step sizes. Higher modes are "washed" out. Figure 11 shows the results which occur if the step size is increased from .0004 hr to .004 hr. If only the final temperatures are required, accurate results can be obtained using this technique. Large CPU savings can occur for large problems.

Table 3. Slab Only Time Constants

Mode	Eigenvalue	Time Constant (hr.)
1	0.403 E-5	248,437.0
2	36.55	.0274
3	141.8	.0071
4	303.0	.0033
5	500.8	.0020
6	711.3	.0014
7	909.1	.0011
8	1070.3	.00093
9	1175.6	.00085
10	1212.1	.00083

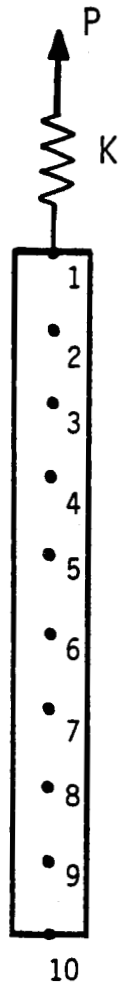

Figure 7. Structural Analogy to One-dimensional Conduction Problem.

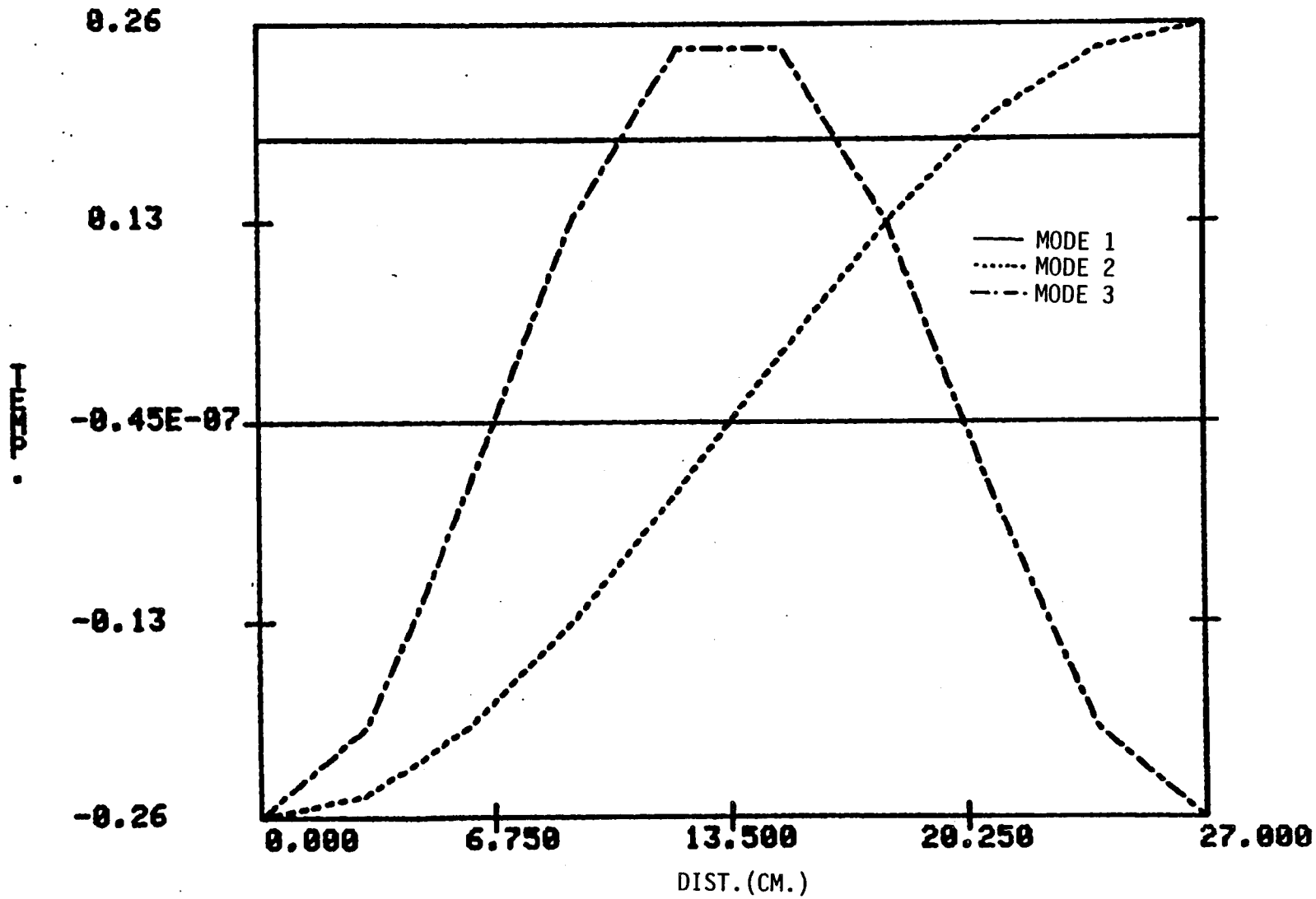

Figure 8. FIRST 3 MODES -- CONDUCTION SLAB ONLY

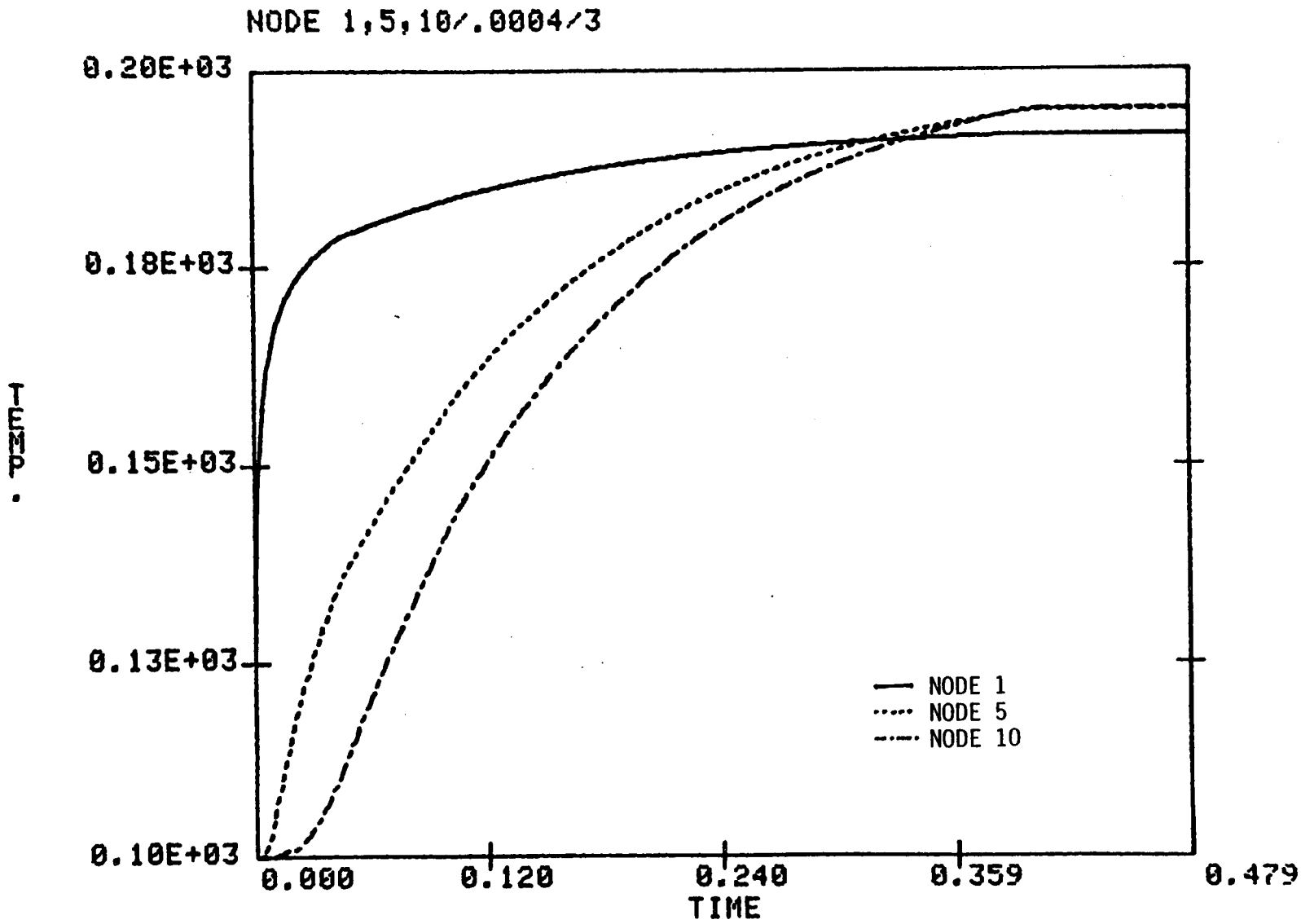

Figure 9. NODAL TEMPERATURE RESPONSES -- MODES DELETED AFTER 3 TIME CONSTANTS

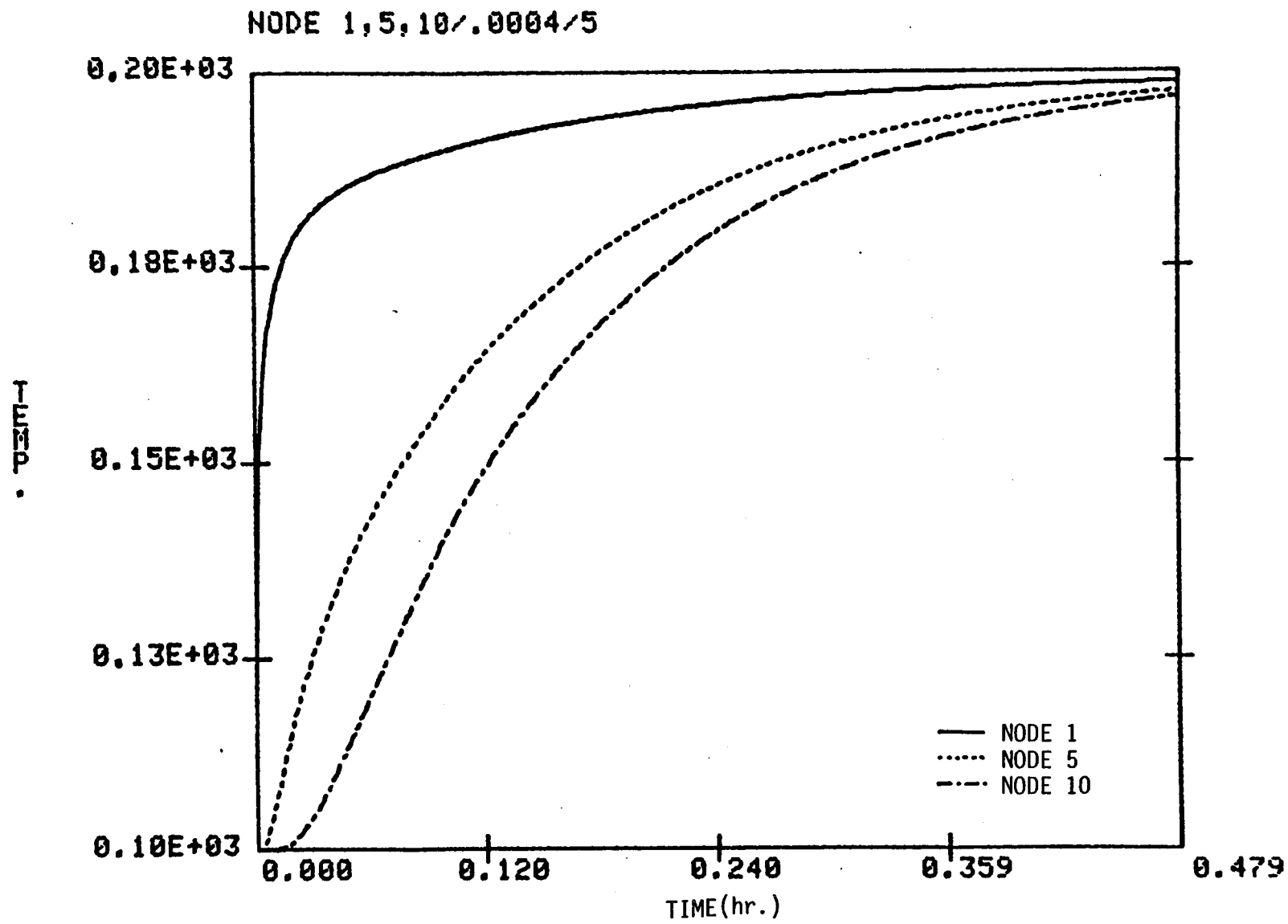

Figure 10. NODAL TEMPERATURE RESPONSES --- MODES DELETED AFTER 5 TIME CONSTANTS

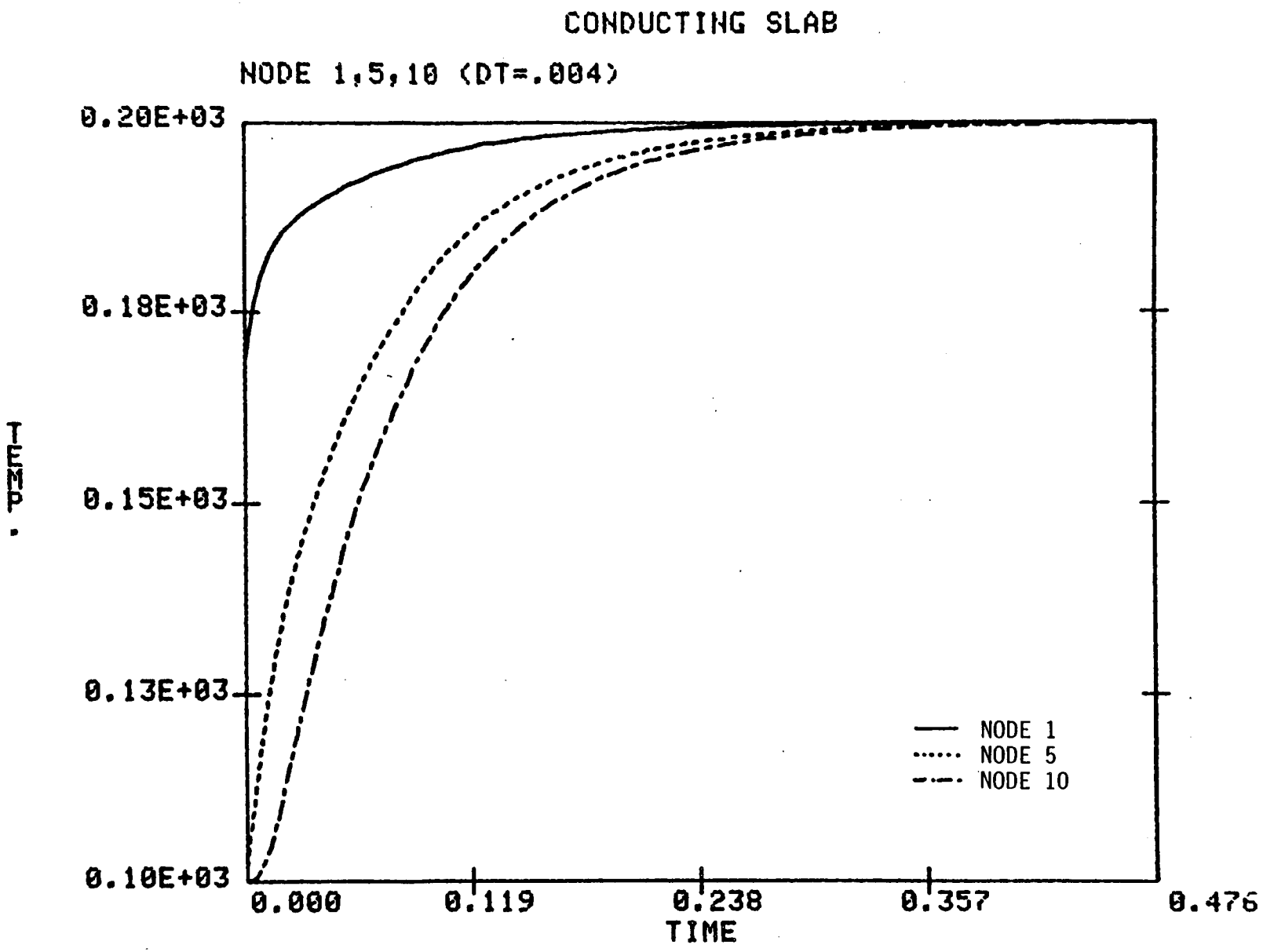

Figure 11. SLAB NODAL TEMPERATURE RESPONSES -- INTEGRATION TIME STEP 10 TIMES LARGER THAN NOMINAL

4.2 JPL ANTENNA PROBLEM

The second problem analyzed using the modal formulation approach is shown in Figure 12. This thermal model was created by Boeing and run using the NTA. The data deck for a typical run of the model is shown in Appendix A. The 55 node model of the pedestal, dish and feeder is given an initial on-orbit temperature of 100°F and solar flux input and nonlinear radiation emission are the main thermal driving forces. Plots of some of the resulting temperature distributions are shown in Figures 13, 14, and 15. These plots are the result of a modal solution run using all 55 modes. Corresponding plots from a coupled solution approach are identical.

The modal eigenvalues and corresponding time constants for the antenna are shown in Table 4. A particularly enlightening way to view the mode shapes is shown in Figure 16. Here, a color graphics display of the first mode shows the symmetric pattern of hot (red, +1°F) and cold (blue, -1°F) regions on the dish. The green region has no appreciable temperature (0°F). The white lines are isothermal lines at 75% of maximum, 50% of maximum and 25% of the maximum temperature excursion. If the antenna is given this temperature distribution, in the absence of external thermal loading, the regions of hot and cold will all exponentially approach 0°F according to the time constant of 160,293 seconds. Likewise, a system with the initial temperature distribution of the 55th mode would exponentially change to 0°F with a time constant of 392 seconds.

As in the previous problem the affect of modal truncation was tested. It was again determined that if all of the structure was to be carefully analyzed, then retention of nearly all of the modes was necessary to give accurate final temperatures. If it was, however, necessary to analyze the

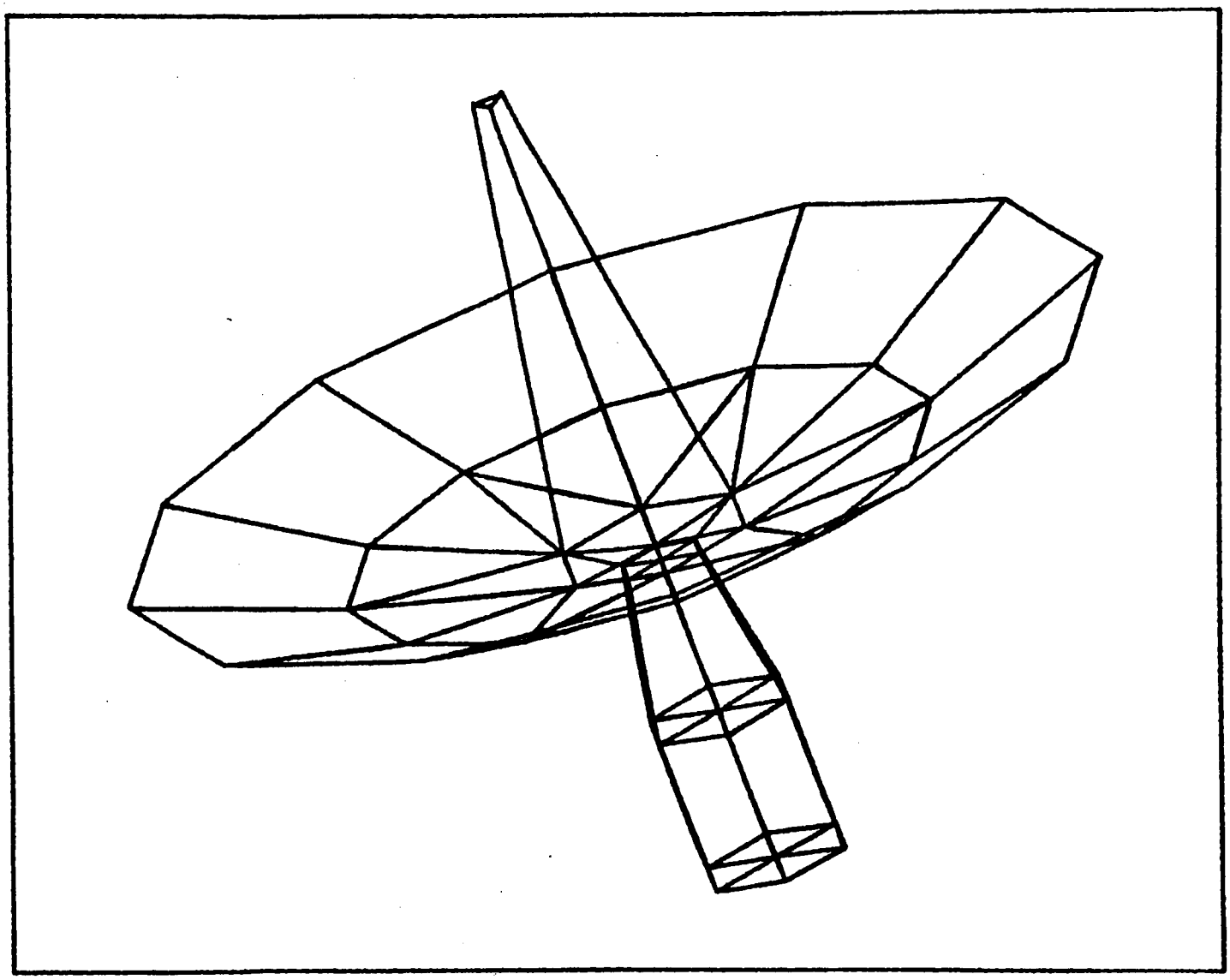

Figure 12. JPL ANTENNA THERMAL MODEL

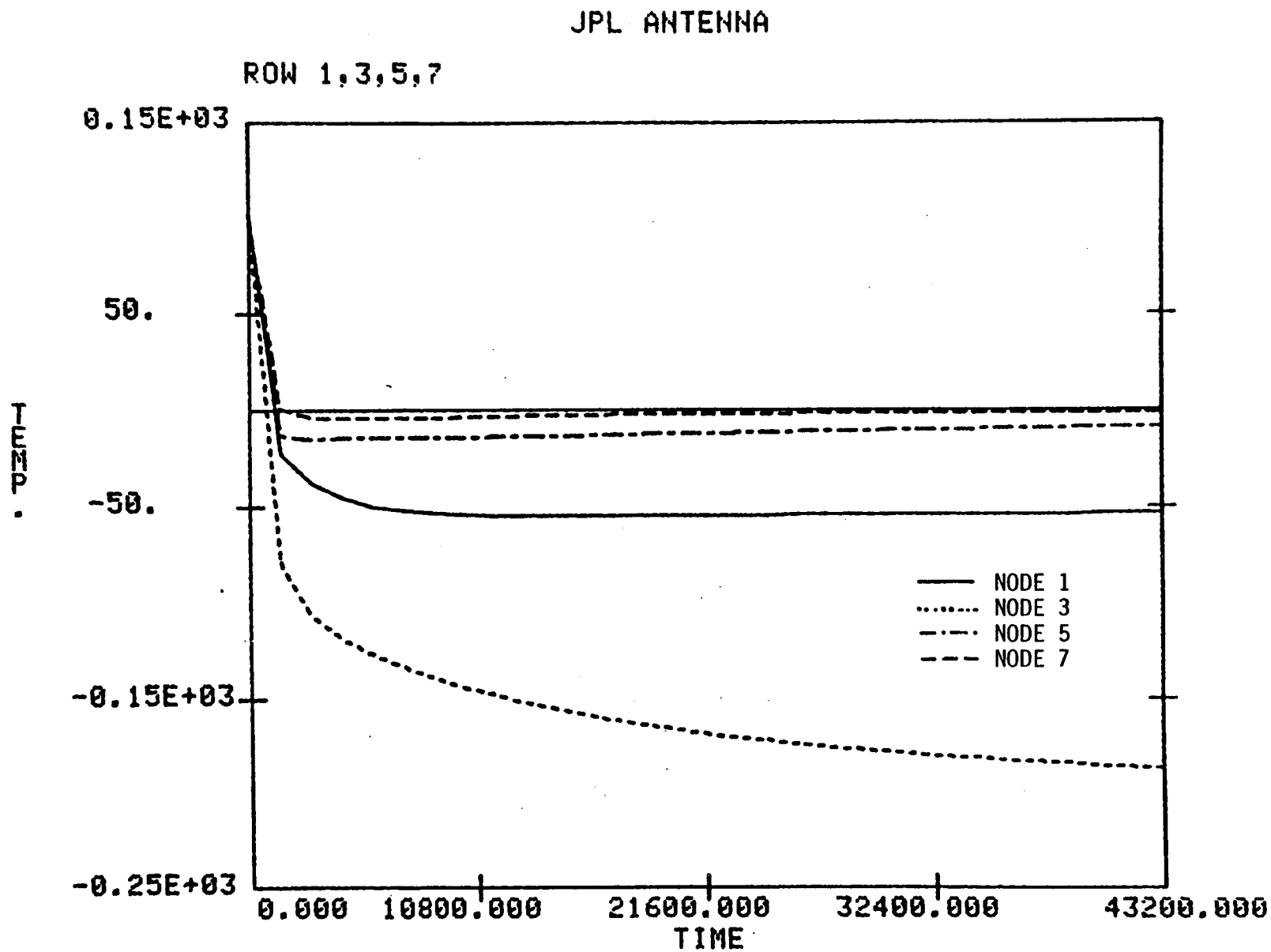

Figure 13. INTERIOR DISH NODAL TEMPERATURE RESPONSES

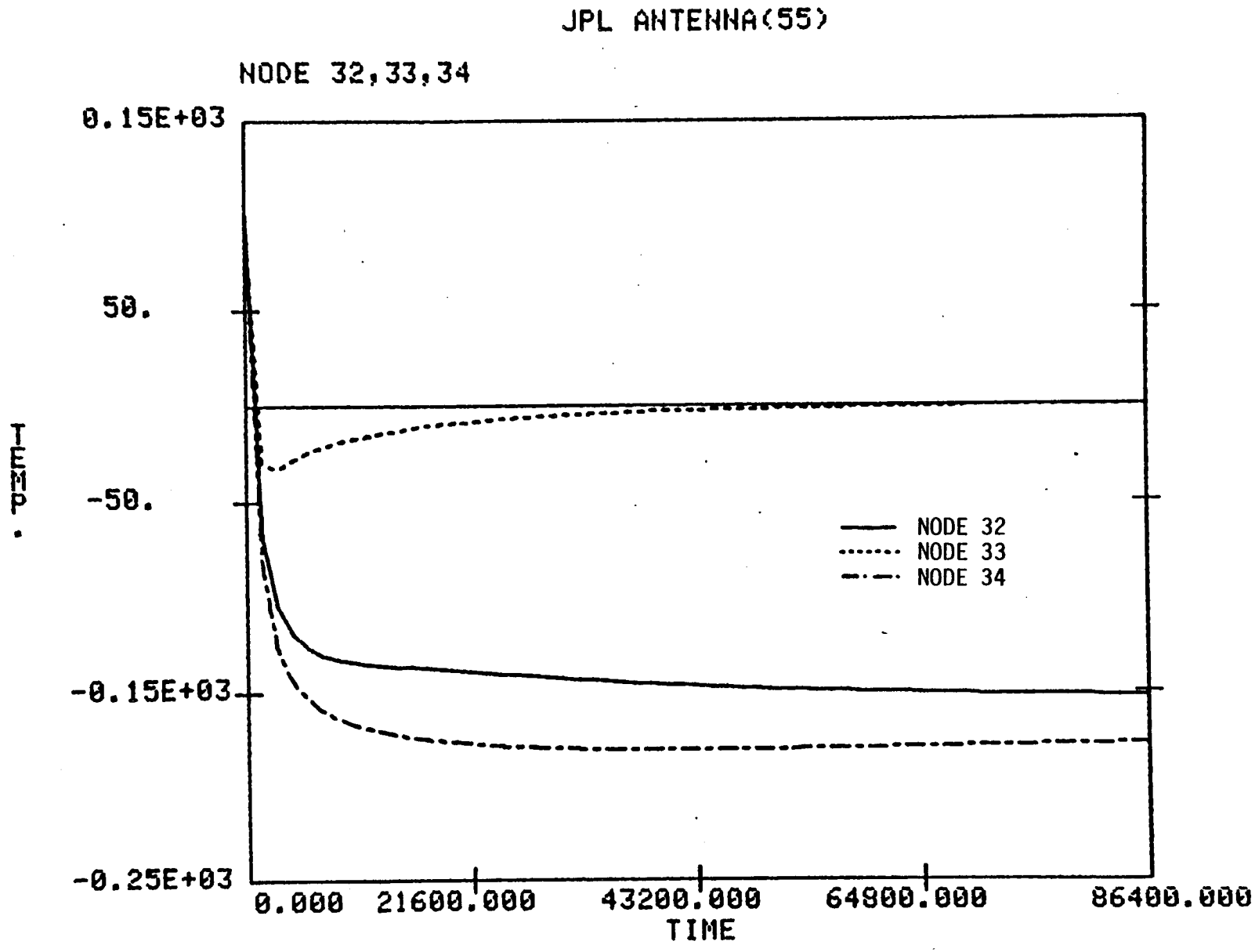

Figure 14. FEEDER NODAL TEMPERATURE RESPONSES

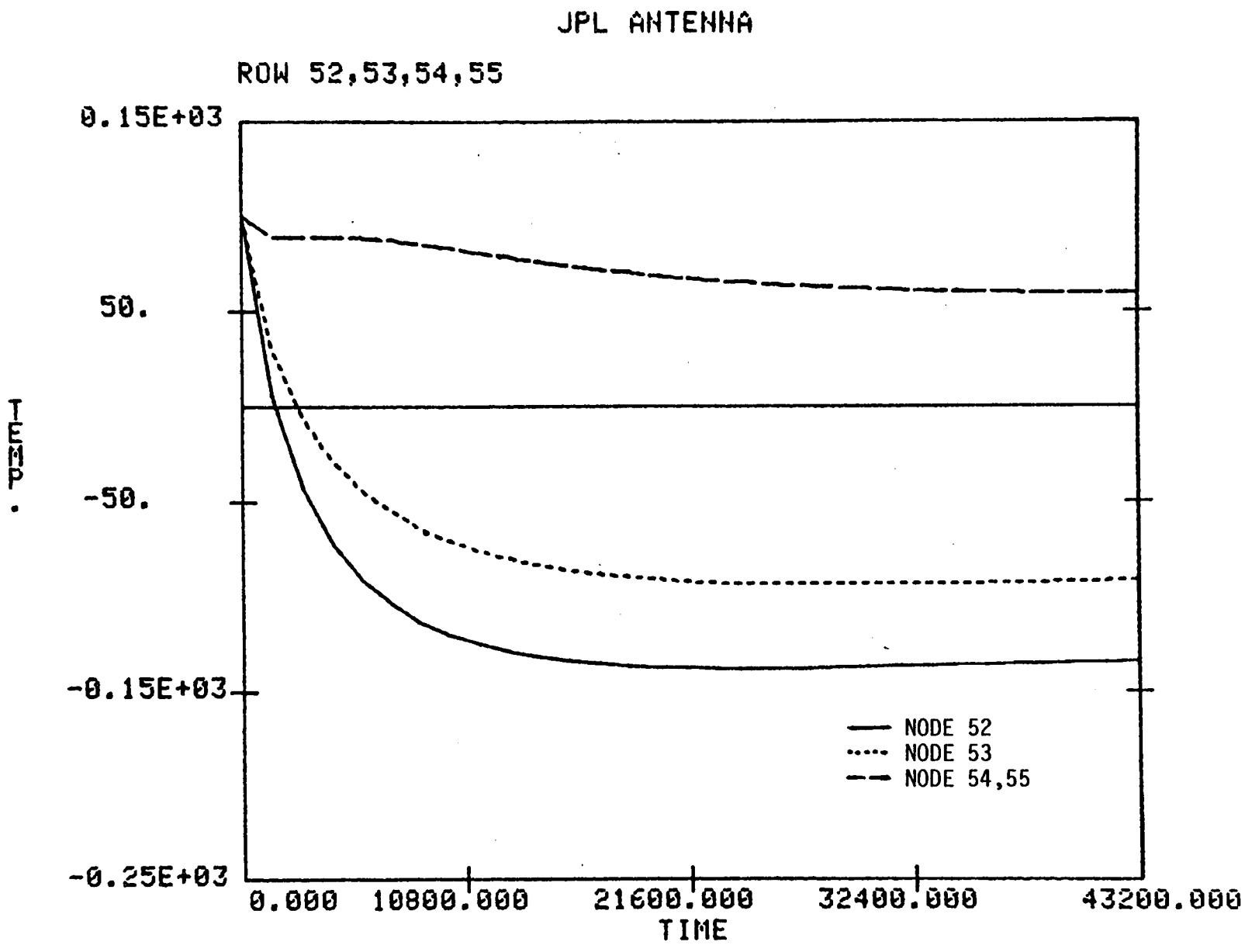

Figure 15. PEDESTAL NODAL TEMPERATURE RESPONSES

Table 4. JPL Antenna Time Constants

Mode	Eigenvalue	Mode	Time Constant
1	0.6238583E-05	1	0.1602928E+06
2	0.1682711E-04	2	0.5942790E+05
3	0.2424366E-04	3	0.4124790E+05
4	0.3373314E-04	4	0.2964444E+05
5	0.4894492E-04	5	0.2043113E+05
6	0.4894838E-04	6	0.2042969E+05
7	0.5309772E-04	7	0.1883320E+05
8	0.5521252E-04	8	0.1811184E+05
9	0.5983795E-04	9	0.1671180E+05
10	0.5983895E-04	10	0.1671152E+05
11	0.6038760E-04	11	0.1655969E+05
12	0.6039083E-04	12	0.1655881E+05
13	0.6131179E-04	13	0.1631008E+05
14	0.6897846E-04	14	0.1449728E+05
15	0.6898009E-04	15	0.1449694E+05
16	0.1190898E-03	16	0.8397024E+04
17	0.1190967E-03	17	0.8396541E+04
18	0.1279474E-03	18	0.7815713E+04
19	0.1330032E-03	19	0.7518619E+04
20	0.1331327E-03	20	0.7511301E+04
21	0.1376842E-03	21	0.7262998E+04
22	0.1378242E-03	22	0.7255622E+04
23	0.1805610E-03	23	0.5538295E+04
24	0.1917642E-03	24	0.5214737E+04
25	0.1917644E-03	25	0.5214733E+04
26	0.2018008E-03	26	0.4955383E+04
27	0.2155735E-03	27	0.4638789E+04
28	0.2365842E-03	28	0.4226825E+04
29	0.2365936E-03	29	0.4226657E+04
30	0.2448175E-03	30	0.4084676E+04
31	0.2448494E-03	31	0.4084143E+04
32	0.2938773E-03	32	0.3402781E+04
33	0.3292675E-03	33	0.3037045E+04
34	0.3703241E-03	34	0.2700337E+04
35	0.3703869E-03	35	0.2699879E+04
36	0.4641326E-03	36	0.2154556E+04
37	0.5059571E-03	37	0.1976452E+04
38	0.6162306E-03	38	0.1622769E+04
39	0.6162323E-03	39	0.1622765E+04
40	0.6842178E-03	40	0.1461523E+04
41	0.6842387E-03	41	0.1461478E+04
42	0.7122986E-03	42	0.1403906E+04
43	0.1047230E-02	43	0.9549000E+03
44	0.1047259E-02	44	0.9548738E+03
45	0.1194648E-02	45	0.8370668E+03
46	0.1255468E-02	46	0.7965157E+03
47	0.1403289E-02	47	0.7126114E+03
48	0.1840473E-02	48	0.5433386E+03
49	0.1840488E-02	49	0.5433342E+03
50	0.2192668E-02	50	0.4560654E+03
51	0.2192704E-02	51	0.4560580E+03
52	0.2298775E-02	52	0.4350142E+03
53	0.2486103E-02	53	0.4022360E+03
54	0.2486168E-02	54	0.4022254E+03
55	0.2550800E-02	55	0.3920338E+03

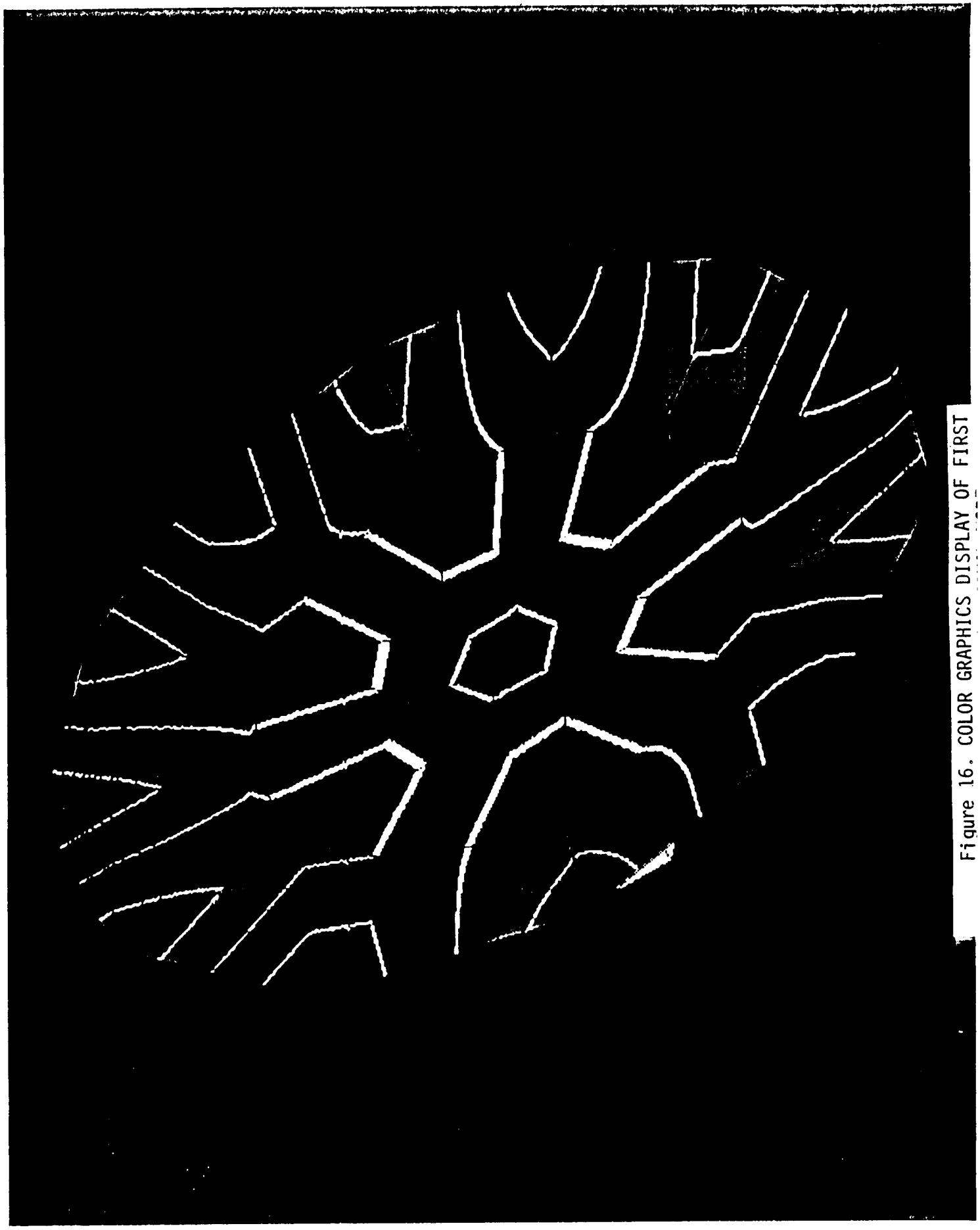

Figure 16. COLOR GRAPHICS DISPLAY OF FIRST

pedestal only, then the last 19 modes could be thrown out with no appreciable accuracy lost. In fact, all modes with mode shapes where the pedestal has essentially zero maximums can be discarded. Accurate results are still obtained as shown in Figure 17. Table 5 gives a simple classification of each thermal mode, displaying the part which has the maximum temperature excursion. This is especially relevant in this problem because of the uncoupled nature of the model.

The modal truncation problem in this example is related to the nonlinear radiative exchanges which depend upon the fourth power of the mode shapes. More analysis is required in order to investigate this effect.

Figure 18 displays, for this small thermal problem, the CPU savings incurred by using the modal formulation versus using the full coupled integration approach. Starting with the system matrices created by NTA, the CPU time for the full coupled system solution is 130 seconds. Including the 14 seconds for a full eigenvalue analysis of the problem, the CPU time for the modal solution using all 55 modes is 118. seconds. If one instead uses only 35 modes, the CPU time drops to 79. seconds, a total reduction of 39 percent.

Admittedly, one can draw almost no conclusions from this one simple example, but it is indicative that a great potential may occur for large problems. Likewise, the potential deletion of modes by reconfiguring the boundary conditions as in the last example leads to positive speculation. Further tests and findings are certainly required.

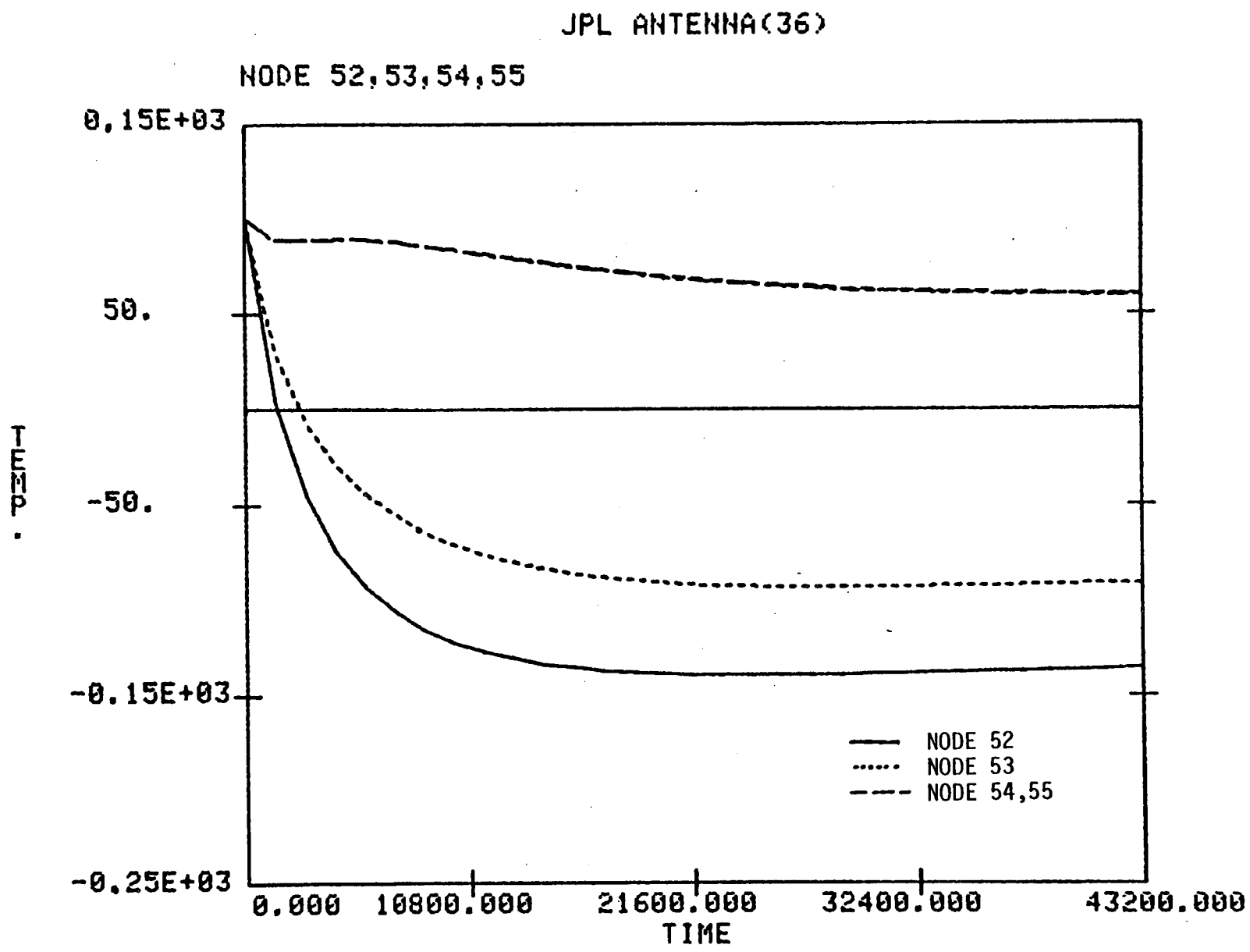

Figure 17. PEDESTAL NODAL TEMPERATURE RESPONSES -- 36 MODE SOLUTION

Table 5. JPL Mode Classification

Mode	Classification	Mode	Classification
1	dish	28	pedestal
2	dish	29	pedestal
3	dish	30	pedestal
4	pedestal	31	pedestal
5	dish	32	pedestal
6	dish	33	pedestal
7	pedestal	34	pedestal
8	pedestal	35	pedestal
9	pedestal	36	pedestal
10	pedestal	37	feeder
11	dish	38	dish
12	dish	39	dish
13	pedestal	40	feeder
14	pedestal	41	feeder
15	pedestal	42	dish
16	dish	43	dish
17	dish	44	dish
18	feeder	45	dish
19	dish	46	dish
20	dish	47	dish
21	pedestal	48	feeder
22	pedestal	49	feeder
23	pedestal	50	feeder
24	dish	51	feeder
25	dish	52	feeder
26	pedestal	53	feeder
27	dish	54	feeder
		55	feeder

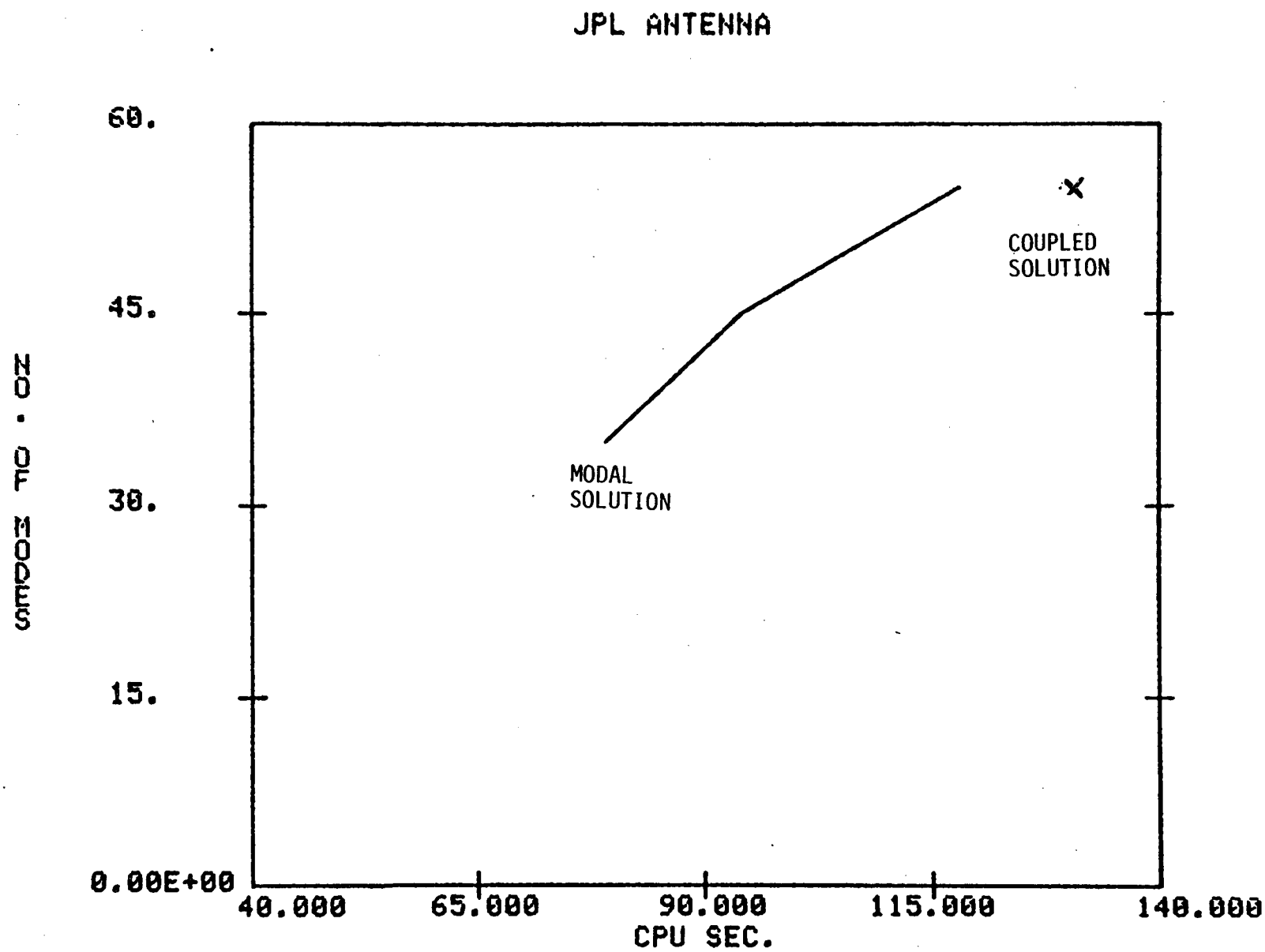

Figure 18. JPL ANTENNA MODEL RUN TIMES

SECTION 5 - CONCLUSION

The modal approach, which has been developed as part of the effort described herein, to the solution of transient thermal problems has been shown to give precise agreement with conventional thermal analysis techniques. Moreover, it has been demonstrated that the fourth-power radiation terms can be treated as part of the right-hand-side of the controlling thermal analysis equation and can thus be easily handled using the modal formulation. The only restriction in the modal approach is that the heat capacitance and conductive matrices must be constant over the temperature range covered by the particular transient of interest.

The results obtained by the sample problems indicate that the modal approach provides a more efficient solution, in terms of computer CPU time, than the standard thermal analysis techniques. It can be anticipated that this improvement in computational efficiency would be more pronounced with larger problems. Moreover, if a general criteria can be developed to allow the truncation of thermal modes which must be used in a thermal transient problem, analogous to the frequency criteria used to truncate modes in a structural response analysis, it may be possible to dramatically reduce the data storage and computer time requirements encountered in the thermal transient analysis of large space structures.

To develop and establish the computational efficiencies offered by the modal approach to thermal transient analysis, additional effort is required and warranted. This effort should address the modal solution of typical large model thermal transient problems and the determination of a criteria which could be used to truncate the number of thermal modes which must be used in these analyses. It is also anticipated that the modal solution may be useful in

providing additional insight into the thermal behavior of large space structures.

APPENDIX A - JPL ANTENNA THERMAL NASTRAN DATA DECK

```
ID NTA, JPL 30 METER DIAMETER ANTENNA
SOL 59
DIAG 8,14,35
DIAG 5,6
TIME 10
ALTER 96
READ HKDD,HBDD,,,DYNAMICS,,CASECC/LAMA,PHIA,MI,OEIGS/MODES/
S,N,NEIGV $
OFP LAMA,OEIGS// $
$MATPRN PHIA// $
VDR CASECC,HEQEXIN,HUSETD,PHIA,LAMA,,/OPHIA,/REIG/DIRECT/0/S,N,NOH/
 S,N,NOPRT/1 $
OFP OPHIA// $
OUTPUT4 HBDD,HKDD,PHIA,HPDT,//-1/11 $
ENDALTER
READ 9
CEND
TITLE=JPL 30-M DEP ANT, THERMAL,TRANS,CONST QVECT
SUBTITLE=GEO,SOLAR ONLY, ECLIPTIC PLANE,EARTH-FACING, 72,7200,86400 SEC
$ 72 SEC TIME STEP,7200 SEC OUT INT (30 DEG),86400 SEC TOT (ONE ORBIT)
$ LENGTH UNITS ARE INCHES
THERMAL=ALL
IC=3
METHOD=700
TSTEP=1
DLOAD=60
BEGIN BULK
EIGR    700     MGIV    0.      1.              55      55      1.E-4   +EIG
+EIG    MASS
CORD2R  2               0.      0.      0.      0.      0.      1.0     +CR
+CR     1.0     0.      1.
CORD2C  1       2       0.      0.      0.      0.      0.      1.0     +CC
+CC     1.0     0.      0.
GRDSET          1                               2
PARAM   SIGMA   3.304-15
PARAM   TABS    460.
GRID     1              0.      0.      0.
GRID     2              118.1   0.      5.91
GRID     3              118.1   60.     5.91
GRID     4              118.1   120.    5.91
GRID     5              118.1   180.    5.91
GRID     6              118.1   240.    5.91
GRID     7              118.1   300.    5.91
GRID     8              354.33  0.      53.15
GRID     9              354.33  30.     53.15
GRID     10             354.33  60.     53.15
GRID     11             354.33  90.     53.15
GRID     12             354.33  120.    53.15
GRID     13             354.33  150.    53.15
```

```
GRID     14              354.33  180.    53.15
GRID     15              354.33  210.    53.15
GRID     16              354.33  240.    53.15
GRID     17              354.33  270.    53.15
GRID     18              354.33  300.    53.15
GRID     19              354.33  330.    53.15
GRID     20              590.55  0.      147.64
GRID     21              590.55  30.     147.64
GRID     22              590.55  60.     147.64
GRID     23              590.55  90.     147.64
GRID     24              590.55  120.    147.64
GRID     25              590.55  150.    147.64
GRID     26              590.55  180.    147.64
GRID     27              590.55  210.    147.64
GRID     28              590.55  240.    147.64
GRID     29              590.55  270.    147.64
GRID     30              590.55  300.    147.64
GRID     31              590.55  330.    147.64
GRID     32              19.69   0.      590.55
GRID     33              19.69   120.    590.55
GRID     34              19.69   240.    590.55
GRID     35              0.      0.      -20.
GRID     36              50.     0.      -20.
GRID     37              50.     60.     -20.
GRID     38              50.     120.    -20.
GRID     39              50.     180.    -20.
GRID     40              50.     240.    -20.
GRID     41              50.     300.    -20.
GRID     42              0.      0.      -220.
GRID     43              90.     0.      -220.
GRID     44              90.     60.     -220.
GRID     45              90.     120.    -220.
GRID     46              90.     180.    -220.
GRID     47              90.     240.    -220.
GRID     48              90.     300.    -220.
GRID     49              0.      0.      -420.
GRID     50              90.     0.      -420.
GRID     51              90.     60.     -420.
GRID     52              90.     120.    -420.
GRID     53              90.     180.    -420.
GRID     54              90.     240.    -420.
GRID     55              90.     300.    -420.
$ TWO-DIGIT ID ELEMENTS ARE BODY (STRUCTURAL ELEMENTS)
$ 100 SERIES ELEMENTS ARE HEAT BOUNDARY ELEMENTS, NEG SIDE, HEAT IN
$ 200 SERIES ELEMENTS ARE HEAT BOUNDARY ELEMENTS, NEG SIDE, HEAT OUT
$ 300 SERIES ELEMENTS ARE HEAT BOUNDARY ELEMENTS, POS SIDE, HEAT IN
CBAR     38      30      2       32      26
CBAR     39      30      4       33      30
CBAR     40      30      6       34      22
CBAR    71       3         2      36       26
CBAR    72       3         3      37       28
```

CBAR	73	3	4	38	30	
CBAR	74	3	5	39	20	
CBAR	75	3	6	40	22	
CBAR	76	3	7	41	24	
CQUAD2	25	2	8	20	21	9
CQUAD2	26	2	9	21	22	10
CQUAD2	27	2	10	22	23	11
CQUAD2	28	2	11	23	24	12
CQUAD2	29	2	12	24	25	13
CQUAD2	30	2	13	25	26	14
CQUAD2	31	2	14	26	27	15
CQUAD2	32	2	15	27	28	16
CQUAD2	33	2	16	28	29	17
CQUAD2	34	2	17	29	30	18
CQUAD2	35	2	18	30	31	19
CQUAD2	36	2	19	31	20	8
CQUAD2	41	4	36	37	44	43
CQUAD2	42	4	37	38	45	44
CQUAD2	43	4	38	39	46	45
CQUAD2	44	4	39	40	47	46
CQUAD2	45	4	40	41	48	47
CQUAD2	46	4	41	36	43	48
CQUAD2	47	4	43	44	51	50
CQUAD2	48	4	44	45	52	51
CQUAD2	49	4	45	46	53	52
CQUAD2	50	4	46	47	54	53
CQUAD2	51	4	47	48	55	54
CQUAD2	52	4	48	43	50	55
CTRIA2	1	1	1	2	3	
CTRIA2	2	1	1	3	4	
CTRIA2	3	1	1	4	5	
CTRIA2	4	1	1	5	6	
CTRIA2	5	1	1	6	7	
CTRIA2	6	1	1	7	2	
CTRIA2	7	1	2	8	9	
CTRIA2	8	1	2	9	3	
CTRIA2	9	1	3	9	10	
CTRIA2	10	1	3	10	11	
CTRIA2	11	1	3	11	4	
CTRIA2	12	1	4	11	12	
CTRIA2	13	1	4	12	13	
CTRIA2	14	1	4	13	5	
CTRIA2	15	1	5	13	14	
CTRIA2	16	1	5	14	15	
CTRIA2	17	1	5	15	6	
CTRIA2	18	1	6	15	16	
CTRIA2	19	1	6	16	17	
CTRIA2	20	1	6	17	7	
CTRIA2	21	1	7	17	18	
CTRIA2	22	1	7	18	19	
CTRIA2	23	1	7	19	2	

CTRIA2	24	1	2	19	8		
CTRIA2	37	1	32	33	34		
CTRIA2	53	5	35	37	36		
CTRIA2	54	5	35	38	37		
CTRIA2	55	5	35	39	38		
CTRIA2	56	5	35	40	39		
CTRIA2	57	5	35	41	40		
CTRIA2	58	5	35	36	41		
CTRIA2	59	5	42	44	43		
CTRIA2	60	5	42	45	44		
CTRIA2	61	5	42	46	45		
CTRIA2	62	5	42	47	46		
CTRIA2	63	5	42	48	47		
CTRIA2	64	5	42	43	48		
CTRIA2	65	5	49	51	50		
CTRIA2	66	5	49	52	51		
CTRIA2	67	5	49	53	52		
CTRIA2	68	5	49	54	53		
CTRIA2	69	5	49	55	54		
CTRIA2	70	5	49	50	55		
CHBDY	101	9	AREA3	1	2	3	
CHBDY	102	9	AREA3	1	3	4	
CHBDY	103	9	AREA3	1	4	5	
CHBDY	104	9	AREA3	1	5	6	
CHBDY	105	9	AREA3	1	6	7	
CHBDY	106	9	AREA3	1	7	2	
CHBDY	107	9	AREA3	2	8	9	
CHBDY	108	9	AREA3	2	9	3	
CHBDY	109	9	AREA3	3	9	10	
CHBDY	110	9	AREA3	3	10	11	
CHBDY	111	9	AREA3	3	11	4	
CHBDY	112	9	AREA3	4	11	12	
CHBDY	113	9	AREA3	4	12	13	
CHBDY	114	9	AREA3	4	13	5	
CHBDY	115	9	AREA3	5	13	14	
CHBDY	116	9	AREA3	5	14	15	
CHBDY	117	9	AREA3	5	15	6	
CHBDY	118	9	AREA3	6	15	16	
CHBDY	119	9	AREA3	6	16	17	
CHBDY	120	9	AREA3	6	17	7	
CHBDY	121	9	AREA3	7	17	18	
CHBDY	122	9	AREA3	7	18	19	
CHBDY	123	9	AREA3	7	19	2	
CHBDY	124	9	AREA3	2	19	8	
CHBDY	125	7	AREA4	8	20	21	9
CHBDY	126	7	AREA4	9	21	22	10
CHBDY	127	7	AREA4	10	22	23	11
CHBDY	128	7	AREA4	11	23	24	12
CHBDY	129	7	AREA4	12	24	25	13
CHBDY	130	7	AREA4	13	25	26	14
CHBDY	131	7	AREA4	14	26	27	15

```
CHBDY   132   7    AREA4   15    27    28    16
CHBDY   133   7    AREA4   16    28    29    17
CHBDY   134   7    AREA4   17    29    30    18
CHBDY   135   7    AREA4   18    30    31    19
CHBDY   136   7    AREA4   19    31    20    8
CHBDY   138   60   ELCYL   2     32                      +BDY1
CHBDY   137   10   AREA3   32    33    34
CHBDY   139   60   ELCYL   4     33                      +BDY2
CHBDY   140   60   ELCYL   6     34                      +BDY3
CHBDY   153   11   AREA3   35    37    36
CHBDY   154   11   AREA3   35    38    37
CHBDY   155   11   AREA3   35    39    38
CHBDY   156   11   AREA3   35    40    39
CHBDY   157   11   AREA3   35    41    40
CHBDY   158   11   AREA3   35    36    41
CHBDY   171   60   ELCYL   2     36                      +BDY4
CHBDY   172   60   ELCYL   3     37                      +BDY5
CHBDY   173   60   ELCYL   4     38                      +BDY6
CHBDY   174   60   ELCYL   5     39                      +BDY7
CHBDY   175   60   ELCYL   6     40                      +BDY8
CHBDY   176   60   ELCYL   7     41                      +BDY9
CHBDY   238   62   ELCYL   2     32                      +BDY10
CHBDY   239   62   ELCYL   4     33                      +BDY11
CHBDY   240   62   ELCYL   6     34                      +BDY12
CHBDY   271   62   ELCYL   2     36                      +BDY13
CHBDY   272   62   ELCYL   3     37                      +BDY14
CHBDY   273   62   ELCYL   4     38                      +BDY15
CHBDY   274   62   ELCYL   5     39                      +BDY16
CHBDY   275   62   ELCYL   6     40                      +BDY17
CHBDY   276   62   ELCYL   7     41                      +BDY18
CHBDY   301   90   AREA3   1     3     2
CHBDY   302   90   AREA3   1     4     3
CHBDY   303   90   AREA3   1     5     4
CHBDY   304   90   AREA3   1     6     5
CHBDY   305   90   AREA3   1     7     6
CHBDY   306   90   AREA3   1     2     7
CHBDY   307   90   AREA3   2     9     8
CHBDY   308   90   AREA3   2     3     9
CHBDY   309   90   AREA3   3     10    9
CHBDY   310   90   AREA3   3     11    10
CHBDY   311   90   AREA3   3     4     11
CHBDY   312   90   AREA3   4     12    11
CHBDY   313   90   AREA3   4     13    12
CHBDY   314   90   AREA3   4     5     13
CHBDY   315   90   AREA3   5     14    13
CHBDY   316   90   AREA3   5     15    14
CHBDY   317   90   AREA3   5     6     15
CHBDY   318   90   AREA3   6     16    15
CHBDY   319   90   AREA3   6     17    16
CHBDY   320   90   AREA3   6     7     17
CHBDY   321   90   AREA3   7     18    17
```

CHBDY	322	90	AREA3	7	19	18	
CHBDY	323	90	AREA3	7	2	19	
CHBDY	324	90	AREA3	2	8	19	
CHBDY	325	70	AREA4	8	9	21	20
CHBDY	326	70	AREA4	9	10	22	21
CHBDY	327	70	AREA4	10	11	23	22
CHBDY	328	70	AREA4	11	12	24	23
CHBDY	329	70	AREA4	12	13	25	24
CHBDY	330	70	AREA4	13	14	26	25
CHBDY	331	70	AREA4	14	15	27	26
CHBDY	332	70	AREA4	15	16	28	27
CHBDY	333	70	AREA4	16	17	29	28
CHBDY	334	70	AREA4	17	18	30	29
CHBDY	335	70	AREA4	18	19	31	30
CHBDY	336	70	AREA4	19	8	20	31
CHBDY	337	10	AREA3	32	34	33	
CHBDY	341	8	AREA4	36	43	44	37
CHBDY	342	8	AREA4	37	44	45	38
CHBDY	343	8	AREA4	38	45	46	39
CHBDY	344	8	AREA4	39	46	47	40
CHBDY	345	8	AREA4	40	47	48	41
CHBDY	346	8	AREA4	41	48	43	36
CHBDY	347	8	AREA4	43	50	51	44
CHBDY	348	8	AREA4	44	51	52	45
CHBDY	349	8	AREA4	45	52	53	46
CHBDY	350	8	AREA4	46	53	54	47
CHBDY	351	8	AREA4	47	54	55	48
CHBDY	352	8	AREA4	48	55	50	43
CHBDY	365	11	AREA3	49	51	50	
CHBDY	366	11	AREA3	49	52	51	
CHBDY	367	11	AREA3	49	53	52	
CHBDY	368	11	AREA3	49	54	53	
CHBDY	369	11	AREA3	49	55	54	
CHBDY	370	11	AREA3	49	50	55	
+BDY1					1.0	0.	0.
+BDY2					1.0	0.	0.
+BDY3					1.0	0.	0.
+BDY4					1.0	0.	0.
+BDY5					1.0	0.	0.
+BDY6					1.0	0.	0.
+BDY7					1.0	0.	0.
+BDY8					1.0	0.	0.
+BDY9					1.0	0.	0.
+BDY10					1.0	0.	0.
+BDY11					1.0	0.	0.
+BDY12					1.0	0.	0.
+BDY13					1.0	0.	0.
+BDY14					1.0	0.	0.
+BDY15					1.0	0.	0.
+BDY16					1.0	0.	0.
+BDY17					1.0	0.	0.

```
+BDY18                                  1.0     0.      0.
PTRIA2  1       11      .040    .00185
PQUAD2  2       11      .040    .00185
PBAR    3       13      .6283
PBAR    30      14      .6283
PQUAD2  4       12      .100
PTRIA2  5       12      .100
PHBDY   60              1.0     .8      .4      32.     32.
PHBDY   62              50.27   .8      .4      16.     16.
PHBDY   7                       .88     .28
PHBDY   70                      .8      .4
PHBDY   8                       .8      .4
PHBDY   9                       .88     .28
PHBDY   90                      .8      .4
PHBDY   10                      .8      .4
PHBDY   11                      .8      .4
$ MAT4 11 IS AL
$ MAT4 13 IS AL
MAT4    11      .00208  .021
$ MAT4 12 IS AL
$ MAT4 14 IS AL
MAT4    12      .00208  .021
MAT4    13      .00208  .021
MAT4    14      .00208  .021
RADLST  101     102     103     104     105     106     107     108     +R1
+R1     109     110     111     112     113     114     115     116     +R2
+R2     117     118     119     120     121     122     123     124     +R3
+R3     125     126     127     128     129     130     131     132     +R4
+R4     133     134     135     136     137     153     154     155     +R5
+R5     156     157     158     238     239     240     271     272     +R6
+R6     273     274     275     276     301     302     303     304     +R7
+R7     305     306     307     308     309     310     311     312     +R8
+R8     313     314     315     316     317     318     319     320     +R9
+R9     321     322     323     324     337     341     342     343     +R10
+R10    344     345     346     347     348     349     350     351     +R11
RADMTX  1       0.      0.      0.      0.      0.      0.      0.      +RM1
+R11    352     325     326     327     328     329     330     331     +R12
+R12    332     333     334     335     336     365     366     367     +R13
+R13    368     369     370
+RM1    0.      0.      0.      0.      0.      0.      0.      0.      +RM2
+RM2    0.      0.      0.      0.      0.      0.      0.      0.      +RM3
+RM3    0.      0.      0.      0.      0.      0.      0.      0.      +RM4
+RM4    0.      0.      0.      0.      0.      0.      0.      0.      +RM5
+RM5    0.      0.      0.      0.      223.24  238.37  238.37  0.      +RM6
+RM6    0.      0.      0.      0.      0.      0.      0.      0.      +RM7
+RM7    0.      0.      0.      0.      0.      0.      0.      0.      +RM8
+RM8    0.      0.      0.      0.      0.      0.      0.      0.      +RM9
+RM9    0.      0.      0.      0.      0.      2.015
RADMTX  2       0.      0.      0.      0.      0.      0.      0.      +RM1
+RM1    0.      0.      0.      0.      0.      0.      0.      0.      +RM2
+RM2    0.      0.      0.      0.      0.      0.      0.      0.      +RM3
```

```
+RM3     0.       0.       0.       0.       0.       0.       0.       0.       +RM4
+RM4     0.       0.       0.       0.       0.       0.       0.       0.       +RM5
+RM5     0.       0.       0.       238.37   223.24   238.37   0.       0.       +RM6
+RM6     0.       0.       0.       0.       0.       0.       0.       0.       +RM7
+RM7     0.       0.       0.       0.       0.       0.       0.       0.       +RM8
+RM8     0.       0.       0.       0.       0.       0.       0.       0.       +RM9
+RM9     0.       0.       0.       0.       2.015
RADMTX   3        0.       0.       0.       0.       0.       0.       0.       +RM10
+RM10    0.       0.       0.       0.       0.       0.       0.       0.       +RM11
+RM11    0.       0.       0.       0.       0.       0.       0.       0.       +RM12
+RM12    0.       0.       0.       0.       0.       0.       0.       0.       +RM13
+RM13    0.       0.       0.       0.       0.       0.       0.       0.       +RM14
+RM14    0.       0.       238.37   223.24   238.37   0.       0.       0.       +RM15
+RM15    0.       0.       0.       0.       0.       0.       0.       0.       +RM16
+RM16    0.       0.       0.       0.       0.       0.       0.       0.       +RM17
+RM17    0.       0.       0.       0.       0.       0.       0.       0.       +RM18
+RM18    0.       0.       0.       2.015
RADMTX   4        0.       0.       0.       0.       0.       0.       0.       +RM19
+RM19    0.       0.       0.       0.       0.       0.       0.       0.       +RM20
+RM20    0.       0.       0.       0.       0.       0.       0.       0.       +RM21
+RM21    0.       0.       0.       0.       0.       0.       0.       0.       +RM22
+RM22    0.       0.       0.       0.       0.       0.       0.       0.       +RM23
+RM23    0.       238.37   238.37   223.24   0.       0.       0.       0.       +RM24
+RM24    0.       0.       0.       0.       0.       0.       0.       0.       +RM25
+RM25    0.       0.       0.       0.       0.       0.       0.       0.       +RM26
+RM26    0.       0.       0.       0.       0.       0.       0.       0.       +RM27
+RM27    0.       0.       2.015
RADMTX   5        0.       0.       0.       0.       0.       0.       0.       +RM28
+RM28    0.       0.       0.       0.       0.       0.       0.       0.       +RM29
+RM29    0.       0.       0.       0.       0.       0.       0.       0.       +RM30
+RM30    0.       0.       0.       0.       0.       0.       0.       0.       +RM31
+RM31    0.       0.       0.       0.       0.       0.       0.       0.       +RM32
+RM32    238.37   238.37   223.24   0.       0.       0.       0.       0.       +RM33
+RM33    0.       0.       0.       0.       0.       0.       0.       0.       +RM34
+RM34    0.       0.       0.       0.       0.       0.       0.       0.       +RM35
+RM35    0.       0.       0.       0.       0.       0.       0.       0.       +RM36
+RM36    0.       2.015
RADMTX   6        0.       0.       0.       0.       0.       0.       0.       +RM37
+RM37    0.       0.       0.       0.       0.       0.       0.       0.       +RM38
+RM38    0.       0.       0.       0.       0.       0.       0.       0.       +RM39
+RM39    0.       0.       0.       0.       0.       0.       0.       0.       +RM40
+RM40    0.       0.       0.       0.       0.       0.       0.       223.24   +RM41
+RM41    238.37   238.37   0.       0.       0.       0.       0.       0.       +RM42
+RM42    0.       0.       0.       0.       0.       0.       0.       0.       +RM43
+RM43    0.       0.       0.       0.       0.       0.       0.       0.       +RM44
+RM44    0.       0.       0.       0.       0.       0.       0.       0.       +RM45
+RM45    2.015
RADMTX   7        0.       0.       0.       0.       0.       0.       0.       +RM46
+RM46    0.       0.       0.       0.       0.       0.       0.       0.       +RM47
+RM47    0.       0.       0.       0.       0.       0.       0.       0.       +RM48
+RM48    0.       0.       0.       0.       0.       0.       0.       0.       +RM49
```

+RM49	0.	0.	0.	0.	0.	0.	252.76	274.0	+RM50
+RM50	276.12	0.	0.	0.	0.	0.	0.	0.	+RM51
+RM51	0.	0.	0.	0.	0.	0.	0.	0.	+RM52
+RM52	0.	0.	0.	0.	0.	0.	0.	0.	+RM53
+RM53	0.	0.	0.	0.	0.	0.	0.	2.0695	
RADMTX	8	0.	0.	0.	0.	0.	0.	0.	+RM54
+RM54	0.	0.	0.	0.	0.	0.	0.	0.	+RM55
+RM55	0.	0.	0.	0.	0.	0.	0.	0.	+RM56
+RM56	0.	0.	0.	0.	0.	0.	0.	0.	+RM57
+RM57	0.	0.	0.	0.	0.	252.72	268.13	268.13	+RM58
+RM58	0.	0.	0.	0.	0.	0.	0.	0.	+RM59
+RM59	0.	0.	0.	0.	0.	0.	0.	0.	+RM60
+RM60	0.	0.	0.	0.	0.	0.	0.	0.	+RM61
+RM61	0.	0.	0.	0.	0.	0.	6.056		
RADMTX	9	0.	0.	0.	0.	0.	0.	0.	+RM62
+RM62	0.	0.	0.	0.	0.	0.	0.	0.	+RM63
+RM63	0.	0.	0.	0.	0.	0.	0.	0.	+RM64
+RM64	0.	0.	0.	0.	0.	0.	0.	0.	+RM65
+RM65	0.	0.	0.	0.	274.76	276.12	274.76	0.	+RM66
+RM66	0.	0.	0.	0.	0.	0.	0.	0.	+RM67
+RM67	0.	0.	0.	0.	0.	0.	0.	0.	+RM68
+RM68	0.	0.	0.	0.	0.	0.	0.	0.	+RM69
+RM69	0.	0.	0.	0.	0.	9.0695			
RADMTX	10	0.	0.	0.	0.	0.	0.	0.	+RM70
+RM70	0.	0.	0.	0.	0.	0.	0.	0.	+RM71
+RM71	0.	0.	0.	0.	0.	0.	0.	0.	+RM72
+RM72	0.	0.	0.	0.	0.	0.	0.	0.	+RM73
+RM73	0.	0.	0.	274.76	276.12	274.76	0.	0.	+RM74
+RM74	0.	0.	0.	0.	0.	0.	0.	0.	+RM75
+RM75	0.	0.	0.	0.	0.	0.	0.	0.	+RM76
+RM76	0.	0.	0.	0.	0.	0.	0.	0.	+RM77
+RM77	0.	0.	0.	0.	9.0695				
RADMTX	11	0.	0.	0.	0.	0.	0.	0.	+RM78
+RM78	0.	0.	0.	0.	0.	0.	0.	0.	+RM79
+RM79	0.	0.	0.	0.	0.	0.	0.	0.	+RM80
+RM80	0.	0.	0.	0.	0.	0.	0.	0.	+RM81
+RM81	0.	0.	268.13	252.72	268.13	0.	0.	0.	+RM82
+RM82	0.	0.	0.	0.	0.	0.	0.	0.	+RM83
+RM83	0.	0.	0.	0.	0.	0.	0.	0.	+RM84
+RM84	0.	0.	0.	0.	0.	0.	0.	0.	+RM85
+RM85	0.	0.	0.	6.056					
RADMTX	12	0.	0.	0.	0.	0.	0.	0.	+RM86
+RM86	0.	0.	0.	0.	0.	0.	0.	0.	+RM87
+RM87	0.	0.	0.	0.	0.	0.	0.	0.	+RM88
+RM88	0.	0.	0.	0.	0.	0.	0.	0.	+RM89
+RM89	0.	276.12	252.76	274.0	0.	0.	0.	0.	+RM90
+RM90	0.	0.	0.	0.	0.	0.	0.	0.	+RM91
+RM91	0.	0.	0.	0.	0.	0.	0.	0.	+RM92
+RM92	0.	0.	0.	0.	0.	0.	0.	0.	+RM93
+RM93	0.	0.	9.0695						
RADMTX	13	0.	0.	0.	0.	0.	0.	0.	+RM94

+RM94	0.	0.	0.	0.	0.	0.	0.	0.	+RM95
+RM95	0.	0.	0.	0.	0.	0.	0.	0.	+RM96
+RM96	0.	0.	0.	0.	0.	0.	0.	0.	+RM97
+RM97	274.0	252.76	276.12	0.	0.	0.	0.	0.	+RM98
+RM98	0.	0.	0.	0.	0.	0.	0.	0.	+RM99
+RM99	0.	0.	0.	0.	0.	0.	0.	0.	+RM100
+RM100	0.	0.	0.	0.	0.	0.	0.	0.	+RM101
+RM101	0.	9.0695							
RADMTX	14	0.	0.	0.	0.	0.	0.	0.	+RM102
+RM102	0.	0.	0.	0.	0.	0.	0.	0.	+RM103
+RM103	0.	0.	0.	0.	0.	0.	0.	0.	+RM104
+RM104	0.	0.	0.	0.	0.	0.	0.	268.13	+RM105
+RM105	252.72	268.13	0.	0.	0.	0.	0.	0.	+RM106
+RM106	0.	0.	0.	0.	0.	0.	0.	0.	+RM107
+RM107	0.	0.	0.	0.	0.	0.	0.	0.	+RM108
+RM108	0.	0.	0.	0.	0.	0.	0.	0.	+RM109
+RM109	6.056								
RADMTX	15	0.	0.	0.	0.	0.	0.	0.	+RM110
+RM110	0.	0.	0.	0.	0.	0.	0.	0.	+RM111
+RM111	0.	0.	0.	0.	0.	0.	0.	0.	+RM112
+RM112	0.	0.	0.	0.	0.	0.	276.12	274.76	+RM113
+RM113	274.76	0.	0.	0.	0.	0.	0.	0.	+RM114
+RM114	0.	0.	0.	0.	0.	0.	0.	0.	+RM115
+RM115	0.	0.	0.	0.	0.	0.	0.	0.	+RM116
+RM116	0.	0.	0.	0.	0.	0.	0.	9.0695	
RADMTX	16	0.	0.	0.	0.	0.	0.	0.	+RM117
+RM117	0.	0.	0.	0.	0.	0.	0.	0.	+RM118
+RM118	0.	0.	0.	0.	0.	0.	0.	0.	+RM119
+RM119	0.	0.	0.	0.	0.	276.12	274.76	274.76	+RM120
+RM120	0.	0.	0.	0.	0.	0.	0.	0.	+RM121
+RM121	0.	0.	0.	0.	0.	0.	0.	0.	+RM122
+RM122	0.	0.	0.	0.	0.	0.	0.	0.	+RM123
+RM123	0.	0.	0.	0.	0.	0.	9.0695		
RADMTX	17	0.	0.	0.	0.	0.	0.	0.	+RM124
+RM124	0.	0.	0.	0.	0.	0.	0.	0.	+RM125
+RM125	0.	0.	0.	0.	0.	0.	0.	0.	+RM126
+RM126	0.	0.	0.	0.	268.13	268.13	252.72	0.	+RM127
+RM127	0.	0.	0.	0.	0.	0.	0.	0.	+RM128
+RM128	0.	0.	0.	0.	0.	0.	0.	0.	+RM129
+RM129	0.	0.	0.	0.	0.	0.	0.	0.	+RM130
+RM130	0.	0.	0.	0.	0.	6.056			
RADMTX	18	0.	0.	0.	0.	0.	0.	0.	+RM131
+RM131	0.	0.	0.	0.	0.	0.	0.	0.	+RM132
+RM132	0.	0.	0.	0.	0.	0.	0.	0.	+RM133
+RM133	0.	0.	0.	276.12	274.0	252.76	0.	0.	+RM134
+RM134	0.	0.	0.	0.	0.	0.	0.	0.	+RM135
+RM135	0.	0.	0.	0.	0.	0.	0.	0.	+RM136
+RM136	0.	0.	0.	0.	0.	0.	0.	0.	+RM137
+RM137	0.	0.	0.	0.	9.0695				
RADMTX	19	0.	0.	0.	0.	0.	0.	0.	+RM138
+RM138	0.	0.	0.	0.	0.	0.	0.	0.	+RM139

```
+RM139  0.      0.      0.      0.      0.      0.      0.      0.      +RM140
+RM140  0.      0.      276.12  274.0   252.76  0.      0.      0.      +RM141
+RM141  0.      0.      0.      0.      0.      0.      0.      0.      +RM142
+RM142  0.      0.      0.      0.      0.      0.      0.      0.      +RM143
+RM143  0.      0.      0.      0.      0.      0.      0.      0.      +RM144
+RM144  0.      0.      0.      9.0695
RADMTX  20      0.      0.      0.      0.      0.      0.      0.      +RM145
+RM145  0.      0.      0.      0.      0.      0.      0.      0.      +RM146
+RM146  0.      0.      0.      0.      0.      0.      0.      0.      +RM147
+RM147  0.      268.13  268.13  252.72  0.      0.      0.      0.      +RM148
+RM148  0.      0.      0.      0.      0.      0.      0.      0.      +RM149
+RM149  0.      0.      0.      0.      0.      0.      0.      0.      +RM150
+RM150  0.      0.      0.      0.      0.      0.      0.      0.      +RM151
+RM151  0.      0.      6.056
RADMTX  21      0.      0.      0.      0.      0.      0.      0.      +RM152
+RM152  0.      0.      0.      0.      0.      0.      0.      0.      +RM153
+RM153  0.      0.      0.      0.      0.      0.      0.      0.      +RM154
+RM154  274.76  276.12  274.76  0.      0.      0.      0.      0.      +RM155
+RM155  0.      0.      0.      0.      0.      0.      0.      0.      +RM156
+RM156  0.      0.      0.      0.      0.      0.      0.      0.      +RM157
+RM157  0.      0.      0.      0.      0.      0.      0.      0.      +RM158
+RM158  0.      9.0695
RADMTX  22      0.      0.      0.      0.      0.      0.      0.      +RM159
+RM159  0.      0.      0.      0.      0.      0.      0.      0.      +RM160
+RM160  0.      0.      0.      0.      0.      0.      0.      274.76  +RM161
+RM161  276.12  274.76  0.      0.      0.      0.      0.      0.      +RM162
+RM162  0.      0.      0.      0.      0.      0.      0.      0.      +RM163
+RM163  0.      0.      0.      0.      0.      0.      0.      0.      +RM164
+RM164  0.      0.      0.      0.      0.      0.      0.      0.      +RM165
+RM165  9.0695
RADMTX  23      0.      0.      0.      0.      0.      0.      0.      +RM166
+RM166  0.      0.      0.      0.      0.      0.      0.      0.      +RM167
+RM167  0.      0.      0.      0.      0.      0.      252.72  268.13  +RM168
+RM168  268.13  0.      0.      0.      0.      0.      0.      0.      +RM169
+RM169  0.      0.      0.      0.      0.      0.      0.      0.      +RM170
+RM170  0.      0.      0.      0.      0.      0.      0.      0.      +RM171
+RM171  0.      0.      0.      0.      0.      0.      0.      6.056
RADMTX  24      0.      0.      0.      0.      0.      0.      0.      +RM172
+RM172  0.      0.      0.      0.      0.      0.      0.      0.      +RM173
+RM173  0.      0.      0.      0.      0.      252.76  276.12  274.0   +RM174
+RM174  0.      0.      0.      0.      0.      0.      0.      0.      +RM175
+RM175  0.      0.      0.      0.      0.      0.      0.      0.      +RM176
+RM176  0.      0.      0.      0.      0.      0.      0.      0.      +RM177
+RM177  0.      0.      0.      0.      0.      0.      9.0695
RADMTX  25      0.      0.      0.      0.      0.      0.      0.      +RM178
+RM178  0.      0.      0.      0.      0.      0.      0.      0.      +RM179
+RM179  0.      0.      0.      0.      1195.1  1195.1  1195.1  0.      +RM180
+RM180  0.      0.      0.      0.      0.      0.      0.      0.      +RM181
+RM181  0.      0.      0.      0.      0.      0.      0.      0.      +RM182
+RM182  0.      0.      0.      0.      0.      0.      0.      0.      +RM183
+RM183  0.      0.      0.      0.      0.      21.197
```

RADMTX	26	0.	0.	0.	0.	0.	0.	0.	+RM184
+RM184	0.	0.	0.	0.	0.	0.	0.	0.	+RM185
+RM185	0.	0.	0.	1195.1	1195.1	1195.1	0.	0.	+RM186
+RM186	0.	0.	0.	0.	0.	0.	0.	0.	+RM187
+RM187	0.	0.	0.	0.	0.	0.	0.	0.	+RM188
+RM188	0.	0.	0.	0.	0.	0.	0.	0.	+RM189
+RM189	0.	0.	0.	0.	21.197				
RADMTX	27	0.	0.	0.	0.	0.	0.	0.	+RM190
+RM190	0.	0.	0.	0.	0.	0.	0.	0.	+RM191
+RM191	0.	0.	1195.1	1195.1	1195.1	0.	0.	0.	+RM192
+RM192	0.	0.	0.	0.	0.	0.	0.	0.	+RM193
+RM193	0.	0.	0.	0.	0.	0.	0.	0.	+RM194
+RM194	0.	0.	0.	0.	0.	0.	0.	0.	+RM195
+RM195	0.	0.	0.	21.197					
RADMTX	28	0.	0.	0.	0.	0.	0.	0.	+RM196
+RM196	0.	0.	0.	0.	0.	0.	0.	0.	+RM197
+RM197	0.	1195.1	1195.1	1195.1	0.	0.	0.	0.	+RM198
+RM198	0.	0.	0.	0.	0.	0.	0.	0.	+RM199
+RM199	0.	0.	0.	0.	0.	0.	0.	0.	+RM200
+RM200	0.	0.	0.	0.	0.	0.	0.	0.	+RM201
+RM201	0.	0.	21.197						
RADMTX	29	0.	0.	0.	0.	0.	0.	0.	+RM202
+RM202	0.	0.	0.	0.	0.	0.	0.	0.	+RM203
+RM203	1195.1	1195.1	1195.1	0.	0.	0.	0.	0.	+RM204
+RM204	0.	0.	0.	0.	0.	0.	0.	0.	+RM205
+RM205	0.	0.	0.	0.	0.	0.	0.	0.	+RM206
+RM206	0.	0.	0.	0.	0.	0.	0.	0.	+RM207
+RM207	0.	21.197							
RADMTX	30	0.	0.	0.	0.	0.	0.	0.	+RM208
+RM208	0.	0.	0.	0.	0.	0.	0.	1195.1	+RM209
+RM209	1195.1	1195.1	0.	0.	0.	0.	0.	0.	+RM210
+RM210	0.	0.	0.	0.	0.	0.	0.	0.	+RM211
+RM211	0.	0.	0.	0.	0.	0.	0.	0.	+RM212
+RM212	0.	0.	0.	0.	0.	0.	0.	0.	+RM213
+RM213	21.197								
RADMTX	31	0.	0.	0.	0.	0.	0.	0.	+RM214
+RM214	0.	0.	0.	0.	0.	0.	1195.1	1195.1	+RM215
+RM215	1195.1	0.	0.	0.	0.	0.	0.	0.	+RM216
+RM216	0.	0.	0.	0.	0.	0.	0.	0.	+RM217
+RM217	0.	0.	0.	0.	0.	0.	0.	0.	+RM218
+RM218	0.	0.	0.	0.	0.	0.	0.	21.197	
RADMTX	32	0.	0.	0.	0.	0.	0.	0.	+RM209
+RM209	0.	0.	0.	0.	0.	1195.1	1195.1	1195.1	+RM210
+RM210	0.	0.	0.	0.	0.	0.	0.	0.	+RM211
+RM211	0.	0.	0.	0.	0.	0.	0.	0.	+RM212
+RM212	0.	0.	0.	0.	0.	0.	0.	0.	+RM213
+RM213	0.	0.	0.	0.	0.	0.	21.197		
RADMTX	33	0.	0.	0.	0.	0.	0.	0.	+RM214
+RM214	0.	0.	0.	0.	1195.1	1195.1	1195.1	0.	+RM215
+RM215	0.	0.	0.	0.	0.	0.	0.	0.	+RM216
+RM216	0.	0.	0.	0.	0.	0.	0.	0.	+RM217

+RM217	0.	0.	0.	0.	0.	0.	0.	0.	+RM218
+RM218	0.	0.	0.	0.	0.	21.197			
RADMTX	34	0.	0.	0.	0.	0.	0.	0.	+RM219
+RM219	0.	0.	0.	1195.1	1195.1	1195.1	0.	0.	+RM220
+RM220	0.	0.	0.	0.	0.	0.	0.	0.	+RM221
+RM221	0.	0.	0.	0.	0.	0.	0.	0.	+RM222
+RM222	0.	0.	0.	0.	0.	0.	0.	0.	+RM223
+RM223	0.	0.	0.	0.	21.197				
RADMTX	35	0.	0.	0.	0.	0.	0.	0.	+RM224
+RM224	0.	0.	1195.1	1195.1	1195.1	0.	0.	0.	+RM225
+RM225	0.	0.	0.	0.	0.	0.	0.	0.	+RM226
+RM226	0.	0.	0.	0.	0.	0.	0.	0.	+RM227
+RM227	0.	0.	0.	0.	0.	0.	0.	0.	+RM228
+RM228	0.	0.	0.	21.197					
RADMTX	36	0.	0.	0.	0.	0.	0.	0.	+RM229
+RM229	0.	1195.1	1195.1	1195.1	0.	0.	0.	0.	+RM230
+RM230	0.	0.	0.	0.	0.	0.	0.	0.	+RM231
+RM231	0.	0.	0.	0.	0.	0.	0.	0.	+RM232
+RM232	0.	0.	0.	0.	0.	0.	0.	0.	+RM233
+RM233	0.	0.	21.197						
RADMTX	37								
RADMTX	38	0.	0.	0.	0.	0.	0.	0.	+RM234
+RM234	0.	0.	0.	0.	0.	0.	0.	0.	+RM235
+RM235	155.36	155.36	155.36	155.36	155.36	155.36			
RADMTX	39	0.	0.	0.	0.	0.	0.	0.	+RM236
+RM236	0.	0.	0.	0.	0.	0.	0.	155.36	+RM237
+RM237	155.36	155.36	155.36	155.36	155.36				
RADMTX	40	0.	0.	0.	0.	0.	0.	0.	+RM238
+RM238	0.	0.	0.	0.	0.	0.	155.36	155.36	+RM239
+RM239	155.36	155.36	155.36	155.36					
RADMTX	41	0.	0.	0.	0.	0.	0.	0.	+RM240
+RM240	0.	0.	0.	0.	0.	155.36	155.36	155.36	+RM241
+RM241	155.36	155.36	155.36						
RADMTX	42	0.	0.	0.	0.	0.	0.	0.	+RM242
+RM242	0.	0.	0.	0.	155.36	155.36	155.36	155.36	+RM243
+RM243	155.36	155.36							
RADMTX	43	0.	0.	0.	0.	0.	0.	0.	+RM244
+RM244	0.	0.	0.	155.36	155.36	155.36	155.36	155.36	+RM245
+RM245	155.36								
RADMTX	44								
RADMTX	45								
RADMTX	46								
RADMTX	47	0.	0.	0.	0.	0.	0.	544.77	+RM246
+RM246	0.	0.	0.	0.	544.77	0.	0.	0.	+RM247
+RM247	0.	0.	0.	0.	0.	0.	0.	0.	+RM248
+RM248	0.	0.	0.	0.	0.	0.	0.	0.	+RM249
+RM249	88.58	0.	0.	0.	0.	88.58	0.	0.	+RM250
+RM250	0.	0.	0.	0.					
RADMTX	48	0.	0.	0.	0.	0.	544.77	544.77	+RM251
+RM251	0.	0.	0.	0.	0.	0.	0.	0.	+RM252
+RM252	0.	0.	0.	0.	0.	0.	0.	0.	+RM253

+RM253	0.	0.	0.	0.	0.	0.	0.	88.58	+RM254
+RM254	88.58	0.	0.	0.	0.	0.	0.		
RADMTX	49	0.	0.	0.	0.	0.	544.77	544.77	+RM256
+RM256	0.	0.	0.	0.	0.	0.	0.	0.	+RM257
+RM257	0.	0.	0.	0.	0.	0.	0.	0.	+RM258
+RM258	0.	0.	0.	0.	0.	0.	0.	88.58	+RM259
+RM259	88.58	0.	0.	0.	0.	0.	0.		
RADMTX	50	0.	0.	0.	0.	0.	544.77	544.77	+RM260
+RM261	0.	0.	0.	0.	0.	0.	0.	0.	+RM262
+RM260	0.	0.	0.	0.	0.	0.	0.	0.	+RM261
+RM262	0.	0.	0.	0.	0.	0.	0.	88.58	+RM263
+RM263	88.58	0.	0.	0.	0.	0.	0.		
RADMTX	51	0.	0.	0.	0.	0.	544.77	544.77	+RM264
+RM264	0.	0.	0.	0.	0.	0.	0.	0.	+RM265
+RM265	0.	0.	0.	0.	0.	0.	0.	0.	+RM266
+RM266	0.	0.	0.	0.	0.	0.	0.	88.58	+RM267
+RM267	88.58	0.	0.	0.	0.	0.	0.		
RADMTX	52	0.	0.	0.	0.	0.	544.77	544.77	+RM268
+RM268	0.	0.	0.	0.	0.	0.	0.	0.	+RM269
+RM269	0.	0.	0.	0.	0.	0.	0.	0.	+RM270
+RM270	0.	0.	0.	0.	0.	0.	0.	88.58	+RM271
+RM271	88.58	0.	0.	0.	0.	0.	0.		
RADMTX	53	0.	0.	0.	0.	0.	0.	0.	+RM272
+RM272	0.	0.	0.	0.	0.	0.	0.	0.	+RM273
+RM273	0.	0.	0.	0.	0.	0.	0.	0.	+RM274
+RM274	0.	0.	.4835	0.	0.	0.	0.	0.	+RM275
+RM275	0.								
RADMTX	54	0.	0.	0.	0.	0.	0.	0.	+RM276
+RM276	0.	0.	0.	0.	0.	0.	0.	0.	+RM277
+RM277	0.	0.	0.	0.	0.	0.	0.	0.	+RM278
+RM278	0.	0.	.4835	0.	0.	0.	0.	0.	+RM279
+RM279	0.								
RADMTX	55	0.	0.	0.	0.	0.	0.	0.	+RM280
+RM280	0.	0.	0.	0.	0.	0.	0.	0.	+RM281
+RM281	0.	0.	0.	0.	0.	0.	0.	0.	+RM282
+RM282	0.	0.	.4835	0.	0.	0.	0.	0.	+RM283
+RM283	0.								
RADMTX	56	0.	0.	0.	0.	0.	0.	0.	+RM284
+RM284	0.	0.	0.	0.	0.	0.	0.	0.	+RM285
+RM285	0.	0.	0.	0.	0.	0.	0.	0.	+RM286
+RM286	0.	0.	.4835	0.	0.	0.	0.	0.	+RM287
+RM287	0.								
RADMTX	57	0.	0.	0.	0.	0.	0.	0.	+RM288
+RM288	0.	0.	0.	0.	0.	0.	0.	0.	+RM289
+RM289	0.	0.	0.	0.	0.	0.	0.	0.	+RM290
+RM290	0.	0.	.4835	0.	0.	0.	0.	0.	+RM291
+RM291	0.								
RADMTX	58	0.	0.	0.	0.	0.	0.	0.	+RM292
+RM292	0.	0.	0.	0.	0.	0.	0.	0.	+RM293
+RM293	0.	0.	0.	0.	0.	0.	0.	0.	+RM294
+RM294	0.	0.	.4835	0.	0.	0.	0.	0.	+RM295

```
+RM295  0.
RADMTX  59      0.      0.      0.      0.      0.      0.      0.      +RM296
+RM296  0.      0.      0.      0.      0.      0.      0.      0.      +RM297
+RM297  0.      0.      0.      0.      1274.4  0.      0.      0.      +RM298
+RM298  0.      1274.4  467.28  0.      0.      0.      0.      467.28
RADMTX  60      0.      0.      0.      0.      0.      0.      0.      +RM299
+RM299  0.      0.      0.      0.      0.      0.      0.      0.      +RM300
+RM300  0.      0.      0.      1310.0  0.      0.      0.      0.      +RM301
+RM301  0.      462.3
RADMTX  61      0.      0.      0.      0.      0.      0.      0.      +RM302
+RM302  0.      0.      0.      0.      0.      0.      0.      0.      +RM303
+RM303  0.      0.      1274.4  1274.4  0.      0.      0.      0.      +RM304
+RM304  467.28  467.28
RADMTX  62      0.      0.      0.      0.      0.      0.      0.      +RM305
+RM305  0.      0.      0.      0.      0.      0.      0.      0.      +RM306
+RM306  0.      1274.4  1274.4  0.      0.      0.      0.      467.28  +RM307
+RM307  467.28
RADMTX  63      0.      0.      0.      0.      0.      0.      0.      +RM308
+RM308  0.      0.      0.      0.      0.      0.      0.      0.      +RM309
+RM309  0.      1310.0  0.      0.      0.      0.      0.      462.3
RADMTX  64      0.      0.      0.      0.      0.      0.      0.      +RM310
+RM310  0.      0.      0.      0.      0.      0.      0.      0.      +RM311
+RM311  1274.4  1274.4  0.      0.      0.      0.      467.28  467.28
RADMTX  65      0.      0.      0.      0.      0.      0.      0.      +RM312
+RM312  0.      0.      0.      0.      0.      0.      0.      1274.4  +RM313
+RM313  1274.4  0.      0.      0.      0.      467.28  467.28
RADMTX  66      0.      0.      0.      0.      0.      0.      0.      +RM314
+RM314  0.      0.      0.      0.      0.      0.      0.      1310.0  +RM315
+RM315  0.      0.      0.      0.      0.      462.3
RADMTX  67      0.      0.      0.      0.      0.      0.      0.      +RM316
+RM316  0.      0.      0.      0.      0.      0.      1274.4  1274.4  +RM317
+RM317  0.      0.      0.      0.      467.28  467.28
RADMTX  68      0.      0.      0.      0.      0.      0.      0.      +RM318
+RM318  0.      0.      0.      0.      0.      1274.4  1274.4  0.      +RM319
+RM319  0.      0.      0.      467.28  467.28
RADMTX  69      0.      0.      0.      0.      0.      0.      0.      +RM320
+RM320  0.      0.      0.      0.      0.      1310.0  0.      0.      +RM321
+RM321  0.      0.      0.      462.3
RADMTX  70      0.      0.      0.      0.      0.      0.      0.      +RM322
+RM322  0.      0.      0.      0.      1274.4  1274.4  0.      0.      +RM323
+RM323  0.      0.      467.28  467.28
RADMTX  71      0.      0.      0.      0.      0.      0.      0.      +RM324
+RM324  0.      0.      0.      1274.4  1274.4  0.      0.      0.      +RM325
+RM325  0.      467.28  467.28
RADMTX  72      0.      0.      0.      0.      0.      0.      0.      +RM326
+RM326  0.      0.      0.      1310.0  0.      0.      0.      0.      +RM327
+RM327  0.      462.3
RADMTX  73      0.      0.      0.      0.      0.      0.      0.      +RM328
+RM328  0.      0.      1274.4  1274.4  0.      0.      0.      0.      +RM329
+RM329  167.28  467.28
RADMTX  74      0.      0.      0.      0.      0.      0.      0.      +RM330
```

```
+RM330  0.      1274.4  1274.4  0.      0.      0.      0.      467.28  +RM331
+RM331  467.28
RADMTX  75      0.      0.      0.      0.      0.      0.      0.      +RM332
+RM332  0.      1310.   0.      0.      0.      0.      0.      462.3
RADMTX  76      0.      0.      1274.4  0.      0.      0.      0.      +RM333
+RM333  1274.4  467.28  0.      0.      0.      0.      467.28
RADMTX  77
RADMTX  78
RADMTX  79
RADMTX  80
RADMTX  81
RADMTX  82
RADMTX  83
RADMTX  84
RADMTX  85
RADMTX  86
RADMTX  87
RADMTX  88
RADMTX  89
RADMTX  90
RADMTX  91
RADMTX  92
RADMTX  93
RADMTX  94
RADMTX  95
RADMTX  96
RADMTX  97
RADMTX  98
RADMTX  99
RADMTX  100
RADMTX  101
RADMTX  102
RADMTX  103
RADMTX  104
RADMTX  105
RADMTX  106
RADMTX  107
QVECT   21      8.5917-41       2       3       171     174     175     +Q1
+Q1     176
QVECT   21      8.5417-41       2       3       304     305     306     +Q2
+Q2     307     308     309     313     314     315     316     317     +Q3
+Q3     318     319     320     321     322     323     324     325     +Q4
+Q4     326     329     330     331     332     333     334     335     +Q5
+Q5     336     337
QVECT   21      8.5417-41       2       3       344     345     346     +Q6
+Q6     350     351     352     365     366     367     368     369     +Q7
+Q7     370
QVECT   21      5.7229-41       2       3       327     328
QVECT   21      4.2708-41       2       3       310     312
QVECT   21      5.9792-41       2       3       301     303
QVECT   21      1.3667-41       2       3       138     139     140
```

```
TABLED1 1                                                          +TAB11
TEMPD   3       100.
TABLED1 2                                                          +TAB21
+TAB11  0.      0.      86400.  0.      ENDT
+TAB21  0.      .86603  86400.  .86603  ENDT
TABLED1 3                                                          +TAB31
+TAB31  0.      .5      86400.  .5      ENDT
TLOAD1  60      21                      23
TABLED1 23                                                         +TAB231
+TAB231 0.      1.0     86400.  1.0     ENDT
TSTEP   1       1200     72.     100
ENDDATA
$
```

REFERENCES

1. Frisch, H. P., "Thermally Induced Response of Flexible Structures: A Method for Analysis," J. of Guidance and Control, Vol. 3, No. 1, January - February 1980.

2. Rathjen, K. A., "CAVE: A Computer Code for Two-Dimensional Transient Heating Analysis of Conceptual Thermal Protection Systems for Hypersonic Vehicles," NASA Contractor Report 2897, 1977.

3. MacNeal, R. H., editor, "The Nastran Theoretical Manual (Level 15.0)," NASA SP-221(01).

4. Hwa-Ping Lee, Jackson, C. C., Jr., Nastran Thermal Analyzer - Theory and Application Including A Guide to Modeling Engineering Problems," Volumes 1 and 2, NASA TM X-3503, NASA TM X 3504, April 1977.

5. Anderes, J. R., Norton, M. A., "FLAME Users Manual," to be published November 1981.

6. Anderes, J. R., Norton, M. A., Teleki, C., "OSS-1 Support Structure Modal Survey Test Support, Task IV and V Report: SUNY Instrument Loads Analysis," ORI Tech. Report No. 1572, September 1979.